Nanoparticle-enhanced phase change materials for thermal energy storage: A critical review

Jiaxuan Li[1], Songping Mo[1,2,*], Zicong Zhou[1], Yanping Du[3], Lisi Jia[1,2], Ying Chen[1,2]

1 School of Materials and Energy, Guangdong University of Technology, Guangzhou 510006, China.

2 Guangdong Provincial Key Laboratory on Functional Soft Condensed Matter, Guangdong University of Technology, Guangzhou 510006, China.

3 School of Engineering, Lancaster University, Lancaster LA1 4YW, UK

Abstract: A critical review on nano-enhanced phase change materials (NePCMs) is presented, underscoring the achievements, inconsistencies in reported data, and challenges within the field. The disparate effects of nanoparticles on the modulation of latent heat of phase change materials (PCMs) are comprehensively evaluated. The review delves into the thermal capacity and complex viscosity variations in NePCMs, evidenced by an in-depth mechanistic analysis. Additionally, the review summarizes the current research on the thermal conductivity of NePCMs across solid and liquid states, providing thorough discussions on the underlying principles and mechanisms. It is found that the uniform dispersion and long-term stability of nanoparticles within PCMs are pivotal for consistent thermal performance. While the thermal capacity of NePCMs is generally reduced due to the addition of nanoparticles, although few studies have observed an increase in both latent heat and specific thermal capacity. The incorporation of nanoparticles typically increases the viscosity of NePCMs, which remains intricate due to the variability in nanoparticle characteristics and potential aggregation. Nanoparticles have demonstrated potential in enhancing the thermal conductivity of NePCMs, yet inconsistencies in the mechanisms of Brownian motion and the formation of semi-solid layers are significant concerns. The review also presents the challenges and future research directions in NePCMs research.

[*]Corresponding author. E*mail address*: mosp@ustc.edu (S. Mo)

Keywords: Phase change material; Thermal energy storage; Nanoparticle; NePCM; Latent heat; Thermophysical property

Nomenclature

BM	ball milling	SA	stearic acid
C8	octanol	SDS	sodium dodecyl sulfate
C14	tetradecanol	SEM	scanning electron microscopy
CF	carbon fiber	SWCNT	single-walled carbon nanotube
C_{md}	molecular density constant	T	temperature
CNT	carbon nanotube	t	time scale
c_p	specific heat capacity	U	thermodynamic internal energy
c_v	constant-volume specific heat capacity	UB	ultrasonic bath
D_B	diffusion coefficient of nanoparticles	u	flow rate
DPL	densely packed layer	V	volume
d_f	fractal dimension	w	interfacial phase width
d_r	particle radius	S	entropy
EG	expanded graphite	**Greek letters**	
EGA	expanded glass aggregate	ρ	density
G-22ane	graphene-doped eicosane	ε	weight fraction
G	volume flow rate	α	thermal diffusivity
GNP	graphene nanoplate	σ	correction factor
GO	graphene oxide	μ	dynamic viscosity
H	enthalpy	τ	shear stress
HITEC	KNO_3-$NaNO_2$-$NaNO_3$	τ_p	momentum relaxation time
K	dynamic viscosity	Φ	volume fraction
k_B	Boltzmann constant	ζ	shear strain rate
k	thermal conductivity	$\emptyset_{int}$	the volume fraction of nanoparticles forming clusters
m	mass	Δ	change in parameter
MA	myristic acid	ρ	density
MWCNT	multi-walled carbon nanotube	ε	weight fraction
MS	magnetic stirring	l	average free path of phonons
NePCM	nanoparticle-enhanced PCM	v	phonon group velocity

NG	nano-graphite	η	power law index
p	pressure	**Subscripts**	
P	pumping power	i	interface
PA	palmitic acid	p	particle
PCM	phase change material	nf	nanofluid
PVT	photovoltaic thermal	bf	base fluid
Q	heat transfer capacity	req	request
R_a	radius of gyration		

1. Introduction

The development of effective thermal energy storage (TES) solutions is pivotal for tackling energy efficiency and sustainability issues. TES is categorized into sensible heat storage, latent heat storage, and thermochemical storage, with latent heat storage mediated by phase change materials (PCMs) being the most prevalent due to its high heat storage density and cost-effectiveness [1]. Despite of broad application potential of PCMs, their low thermal conductivity remains a challenge, hindering restraints or thermal performance due to the reduced energy storage rate and ineffective energy utilization. To address this, researchers have explored the approach of enhancing thermal conductivity of PCMs by adding nanoparticles, which can also influence other thermophysical properties of TES systems.

Numerous reviews on nanoparticle-enhanced PCMs (NePCMs) exist, focusing on PCMs like paraffin [2, 3], fatty acids [4], and salt compounds [5], or on applications such as solar energy systems [6, 7], buildings [8], low-temperature systems [9, 10], and textiles [11]. Studies have discussed the effects of different nanomaterials on thermal conductivity and latent heat [12, 13], summarized the thermal conductivity enhancement effect [14], and the impact on phase change temperature, latent heat, and thermal conductivity [15]. However, disparate results on latent heat and thermal conductivity are neglected, and in-depth discussions on the relevant principles or mechanisms are scarce.

Although latent heat is regarded as the dominant reason for the thermal capacity changes in NePCMs [16], there are few investigations on the thermal capacity variations and the in-depth mechanisms in sensible states where phase change doesn't occur. Furthermore, current discussions on viscosity are primarily focused on non-PCM nanofluids [17-20], with the viscosity of NePCMs and mechanisms remaining underexplored.

Reviews on the enhancement of PCM thermal conductivity by nanoparticles typically discuss on the effects of different nanomaterials [14, 21, 22] or the morphology of nanomaterials [23-25], but few summarize results from the perspective of the phase state of the PCM. Since PCMs store thermal energy through phase changes, the thermal conductivity of NePCM in charging/discharging states is crucial for understanding the effects of nanoparticles.

This review aims to offer a comprehensive examination of the literature on NePCMs. It provides a critical analysis of the divergent findings regarding the modulation of latent heat of PCM by nanoparticles, encompassing both enhancement and reduction effects. The review extends its scope to the specific heat capacity, with particular emphasis on the influence on the specific heat capacity of PCMs and a detailed mechanistic analysis. It explores the intricacies of viscosity changes in NePCMs, attributable to the variability in characteristics and aggregation of nanoparticles. Furthermore, the review synthesizes the current state of thermal conductivity research on NePCMs in solid and liquid phases, offering comprehensive discussions on the foundational principles and mechanisms involved.

2. Preparation techniques for NePCMs

2.1 Two-step method

In the two-step method, nanomaterials, including nanoparticles, nanotubes, nanosheets, and nanowires, are firstly synthesized. Subsequently, the obtained nanomaterials are mixed with the PCM through different physical means. A schematic diagram of the two-step method is shown in Fig. 1. During the preparation process, ultrasonic bath (UB), surface modification, ball milling (BM) and magnetic stirring (MS) are employed to facilitate the dispersion of nanoparticles in the PCM, reducing particle sedimentation and aggregation. Typical examples of NePCMs prepared by the two-step method are presented in Table 1.

Table 1 Preparation of NePCMs by the two-step method.

Auxiliary dispersion method	PCM	Nanoparticle	Fraction (wt%)	Melting enthalpy variation	Solidification enthalpy variation	Ref.
UB	Capric acid-Palmitic acid	GNPs	8.0	Slight decline	Slight decline	[27]
UB	RT 22 HC	GNPs	2.0	4.9% reduction	NA	[28]
UB	$Na_2SO_4 \cdot 10H_2O$	Al/C	1.0	1.1% reduction	16.4% reduction	[29]
UB+Surfactant SDS	Stearic acid	TiO_2	0.05-0.3	Slight decline	Slight decline	[30]
UB+Surfactant SDS	Paraffin	TiO_2/Ag	1.0	10.3% increase	12.6% increase	[31]
UB+MS	Potassium nitrate-sodium nitrate eutectic	EG	1.0	7.8% reduction	NA	[32]
UB+MS	SA-acetamide eutectic	MWCNT/ Al_2O_3	1.0/1.0	10.1% increase	NA	[33]
MS	Paraffin	CuO	NA	Decline	Decline	[34]
UB+BM	D-Mannitol	MWCNTs	0.5	3.8% reduction	3.6% reduction	[35]
BM	Inositol	Al_2O_3	1.0	1.0% increase	NA	[36]
		CuO	1.0	14.7% reduction	NA	
BM	Solar salt	CNTs	0.1	4.3% reduction	3.8% reduction	[37]

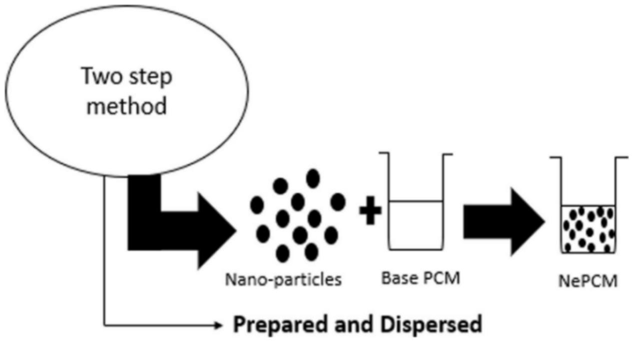

Fig. 1 Preparation of NePCMs by two-step method [26]

Ultrasonication, as shown in Table 1, is a prevalent technique for dispersing nanoparticles in NePCMs, either as a standalone method or in combination with others. This method effectively disaggregates particles, enhancing uniform dispersion. Although there is no standardized protocol for ultrasonic power, mode, or duration, research from National Institute of Standards and Technology and the Center for the Environmental Implications of Nanotechnology recommends using an ice-water or ice-salt bath to control temperature, pulse mode for operation, and selecting container sizes that accommodate the ultrasonic probe without contacting with the walls, thus maximizing exposure to ultrasonic waves and preventing material degradation due to overheating [38].

Jegadheeswaran et al. [39] noted that impact of ultrasound on heat transfer was minimal in the solid phase and became pronounced in the presence of liquid PCM, highlighting its role during natural convection-dominated periods. Shahsavar et al. [40] observed that an ultrasonic field could significantly reduce the melting time of beeswax and further with the addition of copper oxide nanoparticles.

According to Li et al. [41], the ultrasonic field is beneficial to the activation of convective heat transfer processes in the liquid region through acoustic flow and cavitation effects, leading to more uniform nanoparticle dispersion and higher heat transfer efficiency. The so-called acoustic flow effect refers to the gradual decay of energy to form a pressure gradient as ultrasonic vibrations propagate through a liquid medium, driving the fluid flow. This macroscopic flow accelerates the transfer of heat, especially in the bottom region of the melt interface, significantly reducing the melting time. The cavitation effect, on the other hand, refers to the ultrasonic field generating cavitation bubbles in the fluid, which releases localized high temperatures, high pressures and micro-jets during their formation, growth, oscillation and rupture. Firstly, it destroys the thermal boundary layer at the melt interface and reduces its thickness. Secondly, it can enhance convective heat transfer through the impact force during bubble rupture. In addition, it can result in uniform dispersion of nanoparticles and inhibit the agglomeration. Fig. 2 shows the progression of the melting front in both pristine PCMs and their nanoparticle-enhanced counterparts when subjected to ultrasonic fields. The introduction of nanoparticles in conjunction with ultrasonic stimulation accelerated the advancement of the melting front and the higher the ultrasonic power, the faster the melting. For example, a 48 W of ultrasound field reduced the melting time by 57.5% for pure PCM and 72.1% for NEPCM. Concurrently, the research discerns atypical liquid distributions, with the melting front changing from a smooth curve to a sloping or wavy one, which is a reflection of enhanced convection. Additionally, an escalation in ultrasonic power intensity amplifies both the bottom acoustic streaming and the top cavitation effects. This augmentation results in the expansion of the melting front from the central region to the periphery, which ultimately leads to the deformation of the melting front.

The two-step preparation method for NePCMs offers advantageous by enabling independent control over nanoparticle synthesis and dispersion. This allows optimization of size, shape, and surface properties before incorporation, thereby enhancing overall performance. It also provides flexibility in tailoring thermophysical properties for specific applications. For example, Liu et al. [29] synthesized Al/C hybrid nanoparticles with a thorn-ball structure by coating hydrothermally produced carbon onto Al particles. The resulting morphology was compatible with the needle-like crystalline structures formed by $Na_2SO_4 \cdot 10H_2O$ during nucleation, promoting the formation of a continuous 3D network that enhanced lattice heat transfer. The addition of 3.0 wt% Al/C increased thermal conductivity by 26.4% at 30 ℃

in the solid state. Shen et al. [42] modified CNTs using ball milling, mechanochemical treatment, and acid oxidation. The treated CNTs became shorter and exhibited increased surface hydroxyl and carboxyl groups, improving interfacial interactions and dispersion in erythritol. Among the methods, acid oxidation proved most effective, with only 0.5 wt% doping, the solidification temperature of erythritol rose from 18.8 ℃ to 58.2 ℃, and both latent heat and phase change temperature remained stable after ten thermal cycles. These tailored NePCMs demonstrate promising potential for solar TES applications.

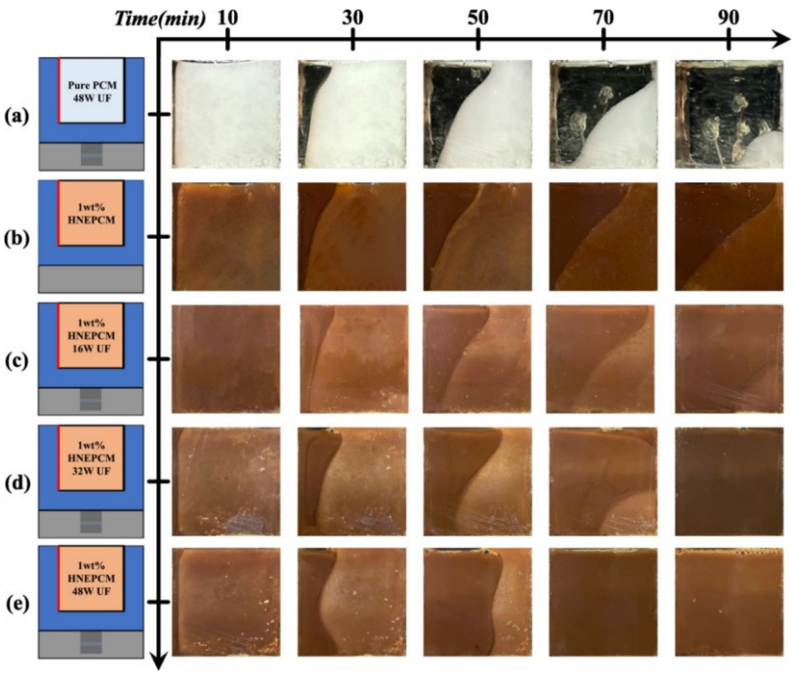

Fig. 2 Evolution of melting front under ultrasonic field: (a) pure PCM 48W UF; (b) NePCM 0 W UF; (c) NePCM 16 W UF; (d) NePCM 32 W UF; (e) NePCM 48 W UF [41]

Enhanced dispersion techniques such as ultrasonication and surfactant use have improved nanoparticle dispersion uniformity and stability in PCMs. Yet, challenges remain, including the long-term stability of nanoparticles in PCMs, which are prone to aggregation and sedimentation. Scaling up the two-step method from laboratory to industrial scale is not trivial and requires adjustments to processing parameters to maintain product consistency.

2.2 One-step method

In contrast to the two-step method, the one-step approach integrates nanoparticle synthesis with their dispersion. This technique employs in-situ synthesis, as demonstrated by Khosravi et al. [43], in which eutectic PCMs of lauric acid and myristic acid (MA) was mixed into fabric, concurrently forming $Al(OH)_3/Al_2O_3$ nanoparticles to develop PCM composite materials, as depicted in Fig. 3. Rezaie et al. [44] utilized a rapid in-situ synthesis method to prepare composite materials with fatty acids as PCMs, polyester fibers as carriers, and $CuFe_2O_4$ nanoparticles as magnetic fillers. Ma et al. [45] synthesized molten salt nanofluids via a one-step process, where metal oxide nanoparticles were in-situ generated from precursors in the molten salt. Liu et al. [46] also in-situ synthesized porous titanium dioxide in molten paraffin, forming composite PCMs after simple stirring and heating. The in situ anchoring effect ensures a uniform distribution of nanoadditives within the composite, maintaining continuous heat transfer pathways.

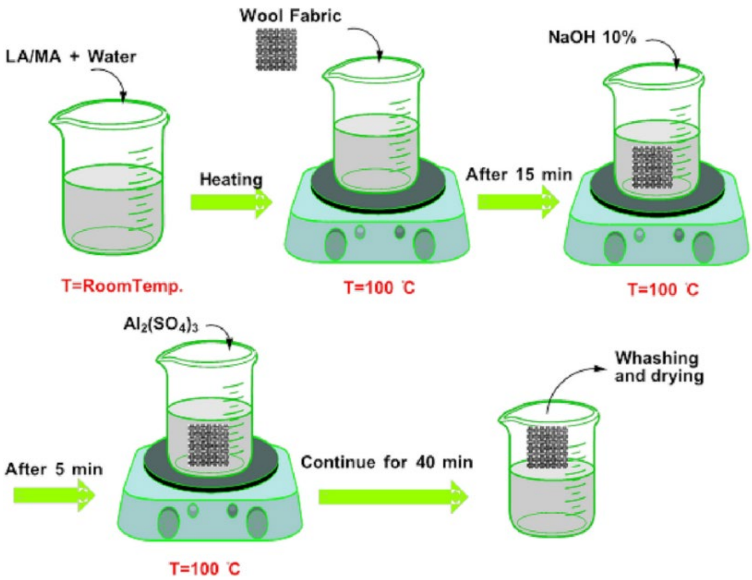

Fig. 3. Preparation of the multi-functional $Al(OH)_3/Al_2O_3$/fatty acids/wool shape-stable composite PCM by in situ synthesis approach [46]

As shown in Fig. 4, Akhiani et al. [47] reduced and functionalized graphene oxide (GO) with long-chain alkylamine and oleylamine, adsorbing palmitic acid (PA) while self-assembling into a three-dimensional structure. The simple one-step self-assembly process avoided the traditional complex impregnation and freeze-drying steps. In addition, due to the simple, controllable, high yield and more consistent production requirements, the one-pot method based on Pickering emulsion template was used by Shang et al. [48] to produce a three-dimensional graphene network of 1-hexadecanol (Fig. 5).

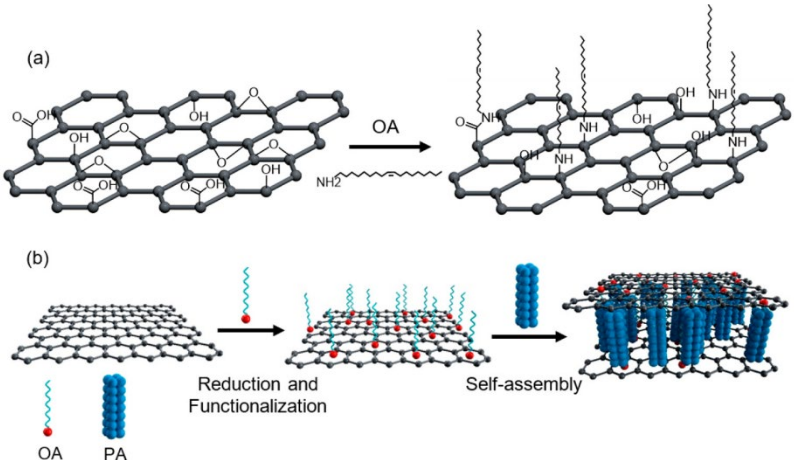

Fig. 4. Schematic illustration of (a) functionalizing GO and (b) one-step self-assembly process [47]

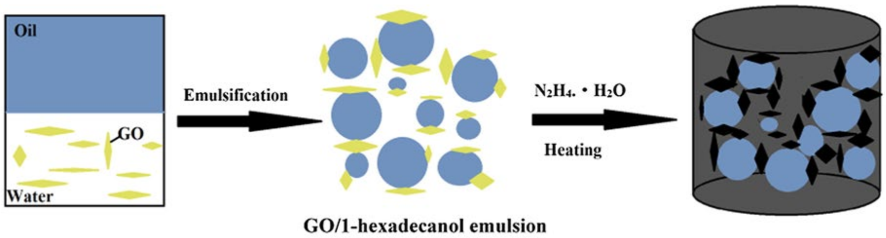

Fig. 5. One-pot method based on Pickering emulsion template for preparation of GO/1-hexadecanol composite [48]

The one-step method for NePCMs preparation simplifies the process by integrating nanoparticle synthesis with their dispersion within the base fluid, potentially enhancing nanoparticle distribution and heat transfer properties. However, this approach sacrifices control over nanoparticle characteristics and presents scalability challenges for industrial production. Improvements in in-situ synthesis have facilitated dispersion and stability through surface modification techniques, yet concerns over the long-term stability of nanoparticles and potential environmental and health impacts during synthesis remain [49].

2.3 Summary in preparation techniques

In summary, NePCM preparation methods can be categorized into one-step and two-step approaches, each with distinct advantages and limitations in nanoparticle dispersion and thermophysical performance. The two-step method is preferred for its scalability and suitability for industrial production, allowing tailored nanocomposites through pre-blending optimization of nanoparticle properties. However, supplementary techniques such as sonication and surface modification are often required to mitigate precipitation and stability issues. In contrast, the one-step method avoids challenges related to nanoparticle handling and dispersion, reducing potential stability risks during synthesis. However, its high cost limits its use to small-scale applications [19], and incomplete reactions may leave residual reactants that degrade NePCM performance [49]. Therefore, the choice between these methods depends on application-specific requirements, balancing scalability, cost, and material performance.

3. Thermal capacity

3.1 Latent heat

Latent heat is widely recognized for its capacity to offer high energy storage density during an isothermal-like phase transition. The solid-liquid transition of PCMs is endothermic, absorbing thermal energy known as melting latent heat. The reverse, liquid-solid transition, is exothermic, releasing heat known as solidification latent heat. Generally, nanoparticle inclusion in PCM leads to a reduction in latent heat, as they displace a portion of the PCM that would otherwise undergo phase change, thereby reducing the overall latent heat [50]. However, empirical data (Table 2) show a more significant decrease compared to the of the effective medium theory, which is a theoretical linear model for quantifying the influence of nanoparticles on the latent heat of NePCMs. This suggests that additional mechanisms may influence the latent heat of NePCMs.

Table 2 Cases of abnormal latent heat reduction in NePCMs.

PCM	Nanoparticle	Fraction (wt%)	Melting enthalpy reduction (%)	Solidification enthalpy reduction (%)	Ref.
Paraffin	Micro-graphite flakes	0.1	1.7	NA	[51]
1-Hexadecanol	CNTs	3.0	5.3	NA	[52]
Lauric acid	MWCNTs	1.0	2.3	1.6	[53]
Paraffin	MWCNTs	0.5	4.7	2.5	[54]
Li_2CO_3-K_2CO_3	SWCNTs	2.5	9.9	NA	[55]
Paraffin	GO	0.3	39.7	NA	[56]
Neopentylene glycol	CuO	0.5	3.1	NA	[57]
MA-SA	CuO	0.2	5.9	5.4	[58]
MA	TiO_2/CuO	1.0	3.6	3.1	[59]
PA	TiO_2	0.5	2.0	NA	[60]
Paraffin	Al_2O_3	5.0	7.0	NA	[61]
Paraffin	Fe_3O_4	5.0	8.3	12.0	[62]
Paraffin	SiO_2	0.5	2.1	3.0	[63]

Wu et al. [64] argued that conventional solid-liquid mixture models are insufficient to evaluate latent heat of nanofluids due to surface and size effects of nanoparticles. They proposed the need for a new theoretical framework but did not pursue this further. Putra et al. [28] found that even a 0.25% addition of graphene in RT 22 HC caused a nearly 5.0 % drop in melting enthalpy. They attributed this reduction to interfacial liquid layering and Brownian motion effects. Specifically, van der Waals forces cause fluid molecules near nanoparticles to form an ordered interfacial layer, introducing strain and weakening molecular bonds. From a Brownian motion perspective, the random movement of nanoparticles disrupts fluid molecule bonding, lowering the energy required for phase change.

However, Zabalegui et al. [65] challenged this explanation by distinguishing two interfacial regions: a densely packed layer (DPL) and a strain layer. They define the interfacial volume fraction (Φ_i) as the ratio of the volume of the interfacial phase (V_i) to the total volume of the nanofluid (V_{nf}):

$$\Phi_{\mathrm{i}} = V_{\mathrm{i}}/V_{\mathrm{nf}} = \Phi_{\mathrm{p}}(V_{\mathrm{i}}/V_{\mathrm{p}}) = \Phi_{\mathrm{p}}(\pi \mathrm{L}\left[(d_{\mathrm{r}} + w)^2 - {d_{\mathrm{r}}}^2\right]/\pi \mathrm{L}{d_{\mathrm{r}}}^2) = \Phi_{\mathrm{p}}(2w/d_{\mathrm{r}} + w^2/{d_{\mathrm{r}}}^2 \quad (1)$$

where Φ is the volume fraction, subscripts i and p represent the interface and particle, respectively; d_{r} is the particle radius and w is the width of the interfacial phase, as shown in Fig. 6.

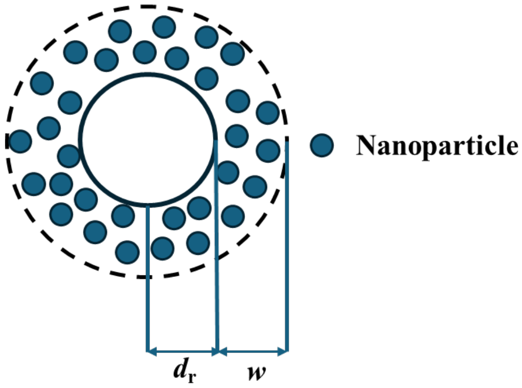

.

Fig. 6 Cross-section of nanofiller with radius d_{r} and interfacial phase width w [65]

The theoretical interfacial volume fraction ($\Phi_{\mathrm{i,req}}$) required to account for the observed latent heat reduction is calculated by Eq. (2)

$$h_{\mathrm{nf}} = \rho_{\mathrm{bf}} h_{\mathrm{bf}} (1 - \Phi_{\mathrm{p}} - \Phi_{\mathrm{i,req}})/\rho_{\mathrm{nf}} \quad (2)$$

where subscripts nf and bf represent the nanofluid and base fluid, respectively. They calculated the theoretical Φ_{i} needed to explain the observed latent heat reduction. Results showed that this value significantly exceeds the effective interfacial volume (limited to ~2 nm DPL), suggesting that interfacial delamination alone cannot account for the observed effects. Due to relatively weak van der Waals forces, the DPL typically extend no more than 2 nm, beyond which the surrounding liquid molecules remain largely unaffected [66, 67], limiting the influence of the strained region.

The authors also assessed the impact of Brownian motion on latent heat reduction. Assuming that w=2 nm, the volume swept by Brownian motion is described by Eq. (3):

$$\pi L\left[(d_{\mathrm{r}} + w)^2 - {d_{\mathrm{r}}}^2\right] + \pi\gamma(d_{\mathrm{r}} + w)^2 \le V \le \pi L\left[(d_{\mathrm{r}} + w)^2 - {d_{\mathrm{r}}}^2\right] + \pi\gamma(2d_{\mathrm{r}} + 2w) \quad (3)$$

where γ represents the average Brownian diffusion length. The time scale required for such Brownian diffusion is calculated by Eq. (4):

$$\gamma = \sqrt{t} \times \sqrt{2k_{\mathrm{B}}T/3\pi\mu d_{\mathrm{r}}} \tag{4}$$

and the actual momentum relaxation time τ_{p} is calculated as:

$$\tau_{\mathrm{p}} = m_{\mathrm{p}}/6\pi\mu d_{\mathrm{r}} \tag{5}$$

where μ is the dynamic viscosity, t is the time scale, k_{B} is the Boltzmann constant, T is temperature, and m is the mass. As shown in Fig. 7, the theoretical diffusion time scale is two orders of magnitude greater than the actual momentum relaxation time, indicating that Brownian motion alone is unlikely to cause substantial reduction in latent heat.

Particle clustering has been suggested as a more plausible mechanism, originally invoked to explain enhanced thermal conductivity (discussed in Section 5). Keblinski et al. [68] noted that nanoparticles tend to agglomerate via van der Waals forces, yet base fluid within aggregates still occupies about 25.0% of the volume. This strained fluid may contribute to unexplained interfacial volume. Prasher et al. [69] modeled clusters as spherical structures with radius of gyration R_{a} (Fig. 8), and Eq. (6) defines the maximum possible R_{a} for fully aggregated nanofluids [70]:

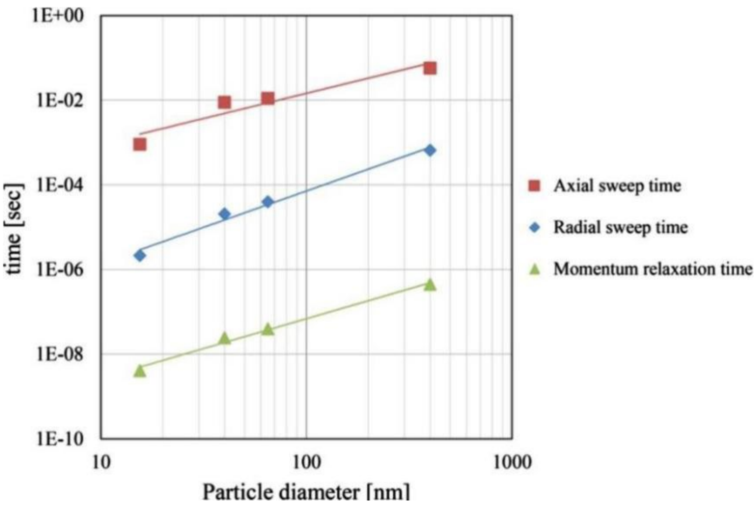

Fig. 7 Comparison of the time scales required by the theory with the corresponding momentum relaxation time scales [65]

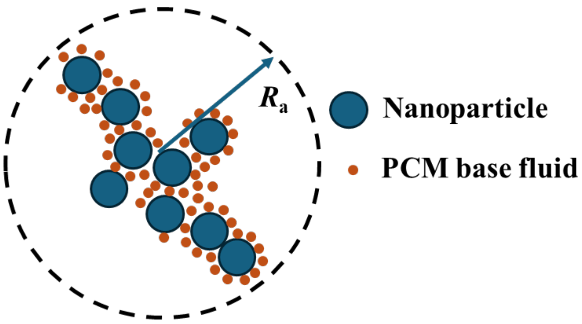

Fig. 8 Assuming that the cluster structure is spherical and its radius of gyration is R_{a} [65]

$$(R_{\mathrm{a}})_{\max} = d_r(\emptyset_{\mathrm{int}})^{1/d_{\mathrm{f}}-3} = d_{\mathrm{r}}(\emptyset_{\mathrm{p}})^{1/d_{\mathrm{f}}-3} \tag{6}$$

where $\emptyset_{\mathrm{int}}$ represent the volume fraction of nanoparticles forming clusters, and d_{f} represent the fractal dimension, commonly taken as 1.8 for nanofluids [69]. Comparing the resulting aggregate volume with the required interfacial volume (Fig. 9) supports the plausibility of this mechanism. However, Jiménez-Galea and Gómez-Merino [71] found this explanation holds best at nanoparticle concentrations below 2.0 vol%. Therefore, future work should employ molecular dynamics simulations or direct thermal measurements to estimate cluster volume fractions and refine understanding of latent heat reduction. Additionally, current findings are limited to specific material combinations; further studies with different nanoparticles and PCM base fluids are needed to assess the generalizability of the mechanism.

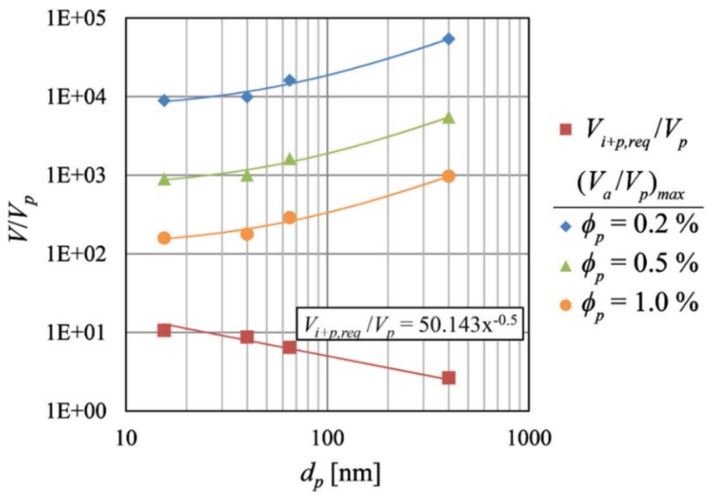

Fig. 9 Plot of maximum cluster volume ratio versus theoretically required interfacial volume ratio for different particle volume fraction [65]

The observed inconsistencies in latent heat modification across NePCMs can be attributed to complex interfacial phenomena and material-specific interactions. Warzoha et al. [72] demonstrated that herringbone graphene nanofibers in paraffin exhibited lower-than-predicted enthalpy reductions, which was speculated to be arisen from compensatory intermolecular forces at the graphene-paraffin interface. Hayat et al. [73] further highlighted that TiO_2-based PCMs retained latent heat more effectively than carbon-based counterparts, which was due to TiO_2's superior dispersion stability and stronger physicochemical bonding with the PCM matrix. On the contrary, carbon-based nanoparticles, despite of their exceptional intrinsic thermal conductivity, suffer from poor dispersion and accelerated paraffin evaporation, reducing effective heat storage capacity [74].

Avid et al. [75] slightly enhanced the latent heat of carbon nanotubes/PCM by surface modification. Similarly, Sheikh et al. [76] investigated the effects of surfactants on graphene nanoflakes in PCMs. Their findings revealed that not all surfactants effectively compensated for latent heat reductions, underscoring the importance of selecting appropriate surfactants. Proper surfactant selection was proven to improve particle compatibility and dispersion, thereby enhancing latent heat retention and overall thermal performance.

Some studies have reported an increase in latent heat following nanoparticle addition, as summarized in Table 3. These findings suggest that nanoparticles can influence phase change behavior through specific mechanisms, offering valuable insights into their potential for improving thermal energy storage systems.

Table 3 Cases of latent heat enhancement in NePCMs

PCM	Nanoparticle	Fraction (wt%)	Melting enthalpy enhancement (%)	Solidification enthalpy enhancement (%)	Ref.
Paraffin	Graphene	Small amount	0.6	2.6	[77]
Paraffin	Carbon quantum dots	1.0	65.1	NA	[78]
Paraffin	GNPs	1.0	19.2	NA	[79]
$Na_2CO_3 \cdot 10H_2O$-$Na_2HPO_4 \cdot 12H_2O$	TiO_2	0.3	6.4	NA	[80]
Paraffin-PA	TiO_2	0.1	12.3	20.1	[81]
KNO_3-$NaNO_2$-$NaNO_3$	TiO_2	0.1	78.0	NA	[82]
Paraffin	CuO	0.3	15.7	NA	[56]
Paraffin	Fe_3O_4	10.0	27.3	NA	[83]
Paraffin	α-Al_2O_3	0.5	14.8	NA	[84]

One key mechanism involves the enhancement of intermolecular forces between nanoparticles and PCMs, which increases the energy required for phase change, consequently, increasing the latent heat. Zabalegui et al. [65] explored the relationship between nanoparticle diameter and latent heat reduction, while Liu et al. [85] demonstrated that smaller particle diameters could increase latent heat due to a greater specific surface area and stronger intermolecular interactions. Sami et al. [86] utilized surfactants like stearoyl lactylate to achieve uniform nanoparticle dispersion at higher concentrations, maximizing latent heat enhancement at 3.0 wt%. Shaikh et al. [87] experimentally and theoretically investigated the latent heat of fusion of CNT-doped paraffin. Among three carbon nano-additives, SWCNTs with the smallest size showed the highest latent heat enhancement (13.0%), followed by MWCNTs (10.1%) and carbon nanofibers (6.8%). The study emphasized the influence of intermolecular forces, ranging from van der Waals interactions to chemical bonds, on latent heat behavior, and is modelled using Leonard-Jones potential theory.

Assuming a 2D arrangement of uniformly distributed CNTs in the PCM. Due to symmetry, a single CNT was used as a representative unit in the theoretical model (Fig. 10). The potential energy function $w(x,y)$ at any coordinate is given by Eq. (7) [88]:

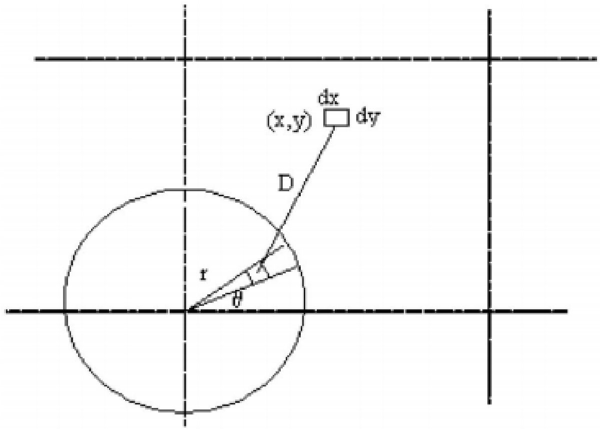

Fig. 10 Physical model for theoretical study [87]

$$w(x,y) = -\rho_{\text{CNT}} c \int_0^{\pi/2} \int_0^r r dr d\theta / [(x - r cos\theta)^2 + (y - r sin\theta)^2]^3 \quad (7)$$

where ρ is the molecule number density and c is a constant (10^{-76} J/m^6). The total interaction forces between nanoparticles and PCM molecules contribute to the latent heat change, expressed in Eq. (8):

$$\Delta H = \rho_{\text{PCM}} \iint_{\text{PCM}} w(x,y) dx dy \quad (8)$$

To align the model with experimental data, a molecular density constant C_{md} was introduced Eq. (9):

$$A = C_{\text{md}} c_{\text{CNT}} \rho_{\text{PCM}} \quad (9)$$

Numerical integration revealed that intermolecular attraction and chemical potential decrease with increasing distance from the nanoparticle surface (Fig. 11), correlating with reduced latent heat (ΔH). The latent energy ratio Q_2/Q_1, defined in Eq. (10), further validated the model:

$$Q_2/Q_1 = 1 + (m_{\text{CNT}}/m_{\text{PCM}} L)\Delta H \quad (10)$$

where L is the latent heat of PCM. As shown in Fig. 12, theoretical predictions closely matched experimental results. Furthermore, latent heat enhancement increased with nanoparticle number density, attributed to higher specific surface area and stronger intermolecular forces for smaller particles.

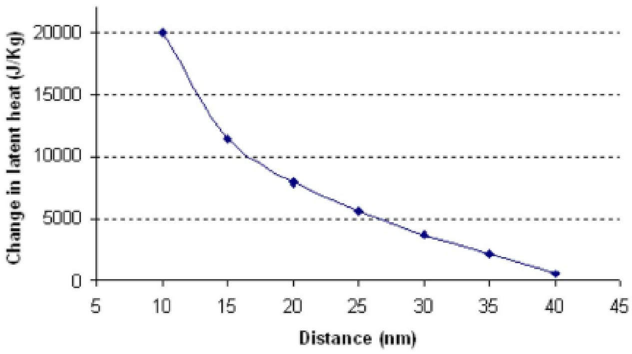

Fig. 11 Plot of latent heat with increasing distance from the nanotube surface [87]

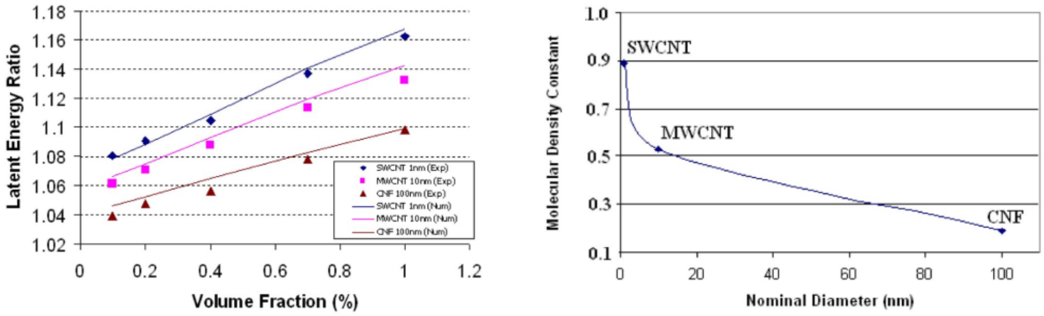

Fig. 12 Plot of (a) predicted vs. experimental values of latent energy ratio and (b) molecular density constant versus nominal diameter [87]

It is worth noting that the model adopted in this study is based on simplified assumptions, i.e., homogeneous dispersion and two-dimensional arrangement, and more research needs to be carried out in the future on the non-homogeneous dispersion and three-dimensional effects that may occur in real composites. In addition, the influence of interfacial effects on latent heat can be further quantified by combining molecular dynamics and macroscopic thermodynamic modelling.

In addition to enhancing intermolecular forces, nanoparticles also act as nucleation sites, promoting crystallinity and lattice order, which further increases latent heat. Liu et al. [89] observed that titanium dioxide nanoparticles increased solidification enthalpy without affecting the melting enthalpy, which was attributed to the promotion of heterogeneous nucleation. Li et al. [77] observed increased solidification and melting latent heat in graphene-doped eicosane (G-22ane), supported by scanning electron microscopy (SEM) images (Fig. 13), showing a denser and smoother sample polycrystalline alkyl layer compared to pure eicosane.

This conclusion was confirmed by the XRD results, where the crystallinity of docosane significantly increased, e.g. the {100} crystallographic peak intensity was enhanced from 733 cps to 1520 cps, thus requiring more energy to disrupt the lattice. Babaei et al. [90] corroborated these findings through molecular dynamics simulations, demonstrating that graphene enhanced directional ordering within a paraffin matrix.

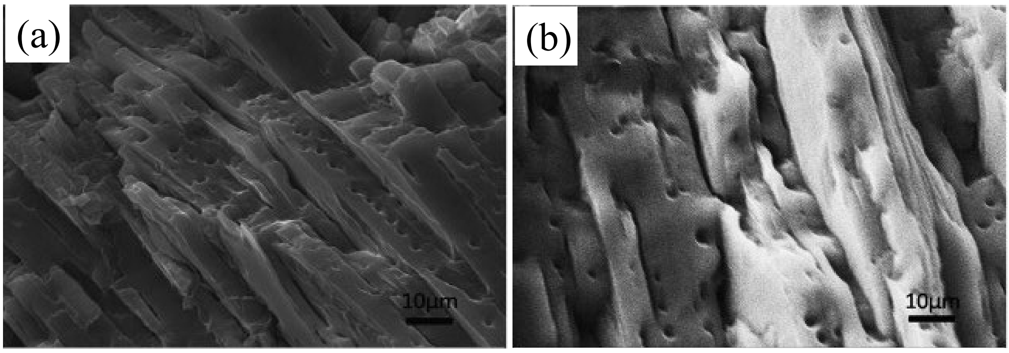

Fig. 13 SEM images of (a) G-22ane and (b) 22ane [77]

However, current research is limited to qualitatively explanation of the relationship between crystallinity and latent heat and lacks quantitative models to predict the effect of nanoparticle content and crystallinity on latent heat. Future refinement of this part of the work would be beneficial for material customization and thus precise modulation of properties.

3.2 Summary in latent heat

In summary, the incorporation of nanoparticles into PCMs can have both positive and negative effects on latent heat, depending on several factors. Rufuss et al. [91] highlighted that these effects were influenced by the nanoparticle type, base PCM characteristics, structural lattice bond arrangements, and dispersion and surface properties of nanoparticles. Moreover, some researchers have emphasized that the mass fraction of nanoparticles plays a crucial role in determining their impacts on latent heat [92]. At low mass fractions, nanoparticles tend to enhance latent heat, but as their fraction increases, they may restrict the movement of PCM molecules, leading to a decrease in latent heat [85, 93, 94]. Yang et al. [95] provided a thermodynamic explanation for the observed latent heat variations using the following equations:

$$\Delta U = T\Delta S - p\Delta V \quad (11)$$

$$\Delta H = \Delta U + V\Delta p \quad (12)$$

Assuming isobaric mixing conditions, the principle of entropy increase suggests that ΔS>0. At low nanoparticle concentrations, partial compatibility between nanoparticles and the PCM may occur. If volume change ΔV is negligible, then $T\Delta S$>$p\Delta V$, leading to ΔU>0 and ΔH>0, which corresponds to an increase in latent heat. However, at higher concentrations, $p\Delta V$ exceeds $T\Delta S$, resulting in ΔU<0 and ΔH<0, thereby reducing latent heat.

To improve prediction accuracy, the latent heat of NePCMs was redefined as follows:

$$\Delta H_{\mathrm{NePCM}} = \sigma\,(k_{\mathrm{NePCM}}\alpha_{\mathrm{PCM}}/k_{\mathrm{PCM}}\alpha_{\mathrm{NePCM}})\Delta H_{\mathrm{PCM}} \quad (13)$$

where α represents thermal diffusivity, k represents thermal conductivity, and σ is a correction factor. The deviations between experimental and calculated values for nanoparticle mass fractions ranging from 1.0 wt% to 10.0 wt% were between 1.3% and 5.7%, indicating good agreement. However, the variation in error across concentrations was not further explained, suggesting that key influencing factors, such as filler dispersion and interfacial thermal resistance, are not fully covered by the current model.

Despite of significant progress in understanding the effects of nanoparticles on latent heat, several challenges remain unresolved. A primary concern is the inconsistency in reported data, with some studies showing increases in latent heat while others report decreases. This variability suggests a complex and incomplete understanding of the relationship between nanoparticles and PCMs. Additionally, the long-term stability of NePCMs remains a challenges, as nanoparticles may settle or aggregate over time, negatively impacting the effective latent heat. Furthermore, there is also a necessity for more comprehensive models that can accurately predict the latent heat of NePCMs under varying conditions, addressing current gaps and inconsistency in experimental and theoretical studies.

3.3 Sensible heat

PCMs can store thermal energy via sensible heat, associated with temperature changes in the solid or liquid phase. Specific heat capacity measures the energy required to raise temperature of a substance by 1 ℃. Fewer studies have been conducted on the specific heat capacity of NePCMs, mainly focusing on molten salt-based PCMs. Three mechanisms are recognized for the enhancement of specific heat in nanofluids: First, higher specific surface energy of nanoparticles intensifies interactions with the surrounding atomic interface, increasing specific heat [96]. Second, the increasing specific surface area of nanoparticles raises interface thermal resistance with liquid molecules, contributing to additional heat storage and higher specific heat [97]. Third, liquid molecules forming a semi-solid layer on particle surfaces (which has been confirmed by molecular dynamics simulations [98] and high-resolution transmission electron microscopy [99]) requires extra energy to disrupt.

3.3.1 Eutectic molten salt based NePCMs

Anomalous increase in specific heat capacity is mostly observed in NePCMs based on eutectic molten salts, as shown in Table 4.

Table 4 Cases of specific heat enhancement in eutectic molten salt NePCMs.

PCM	Nanoparticle	Fraction (wt%)	Solid enhancement (%)	Liquid enhancement (%)	Ref.
Li_2CO_3-K_2CO_3	Graphene	1.5	16.8	18.6	[55]
Li_2CO_3-K_2CO_3	SWCNTs	1.5	18.7	14.4	[55]
Li_2CO_3-K_2CO_3	MWCNTs	1.5	12.4	14.5	[55]
Li_2CO_3-K_2CO_3	C60	1.5	7.1	10.5	[55]
$MgCl_2$-NaCl-KCl	EG-SiO_2	25.0/1.0	136	163	[100]
Li_2CO_3-K_2CO_3	SiO_2	1.0	NA	19.0	[101]
Li_2CO_3-K_2CO_3	5 nm SiO_2	1.0	25.0	24.0	[102]
Li_2CO_3-K_2CO_3	10 nm SiO_2	1.0	29.0	26.0	[102]
Li_2CO_3-K_2CO_3	30 nm SiO_2	1.0	23.0	23.0	[102]
Li_2CO_3-K_2CO_3	60 nm SiO_2	1.0	28.0	26.0	[102]
KNO_3-$NaNO_2$-$NaNO_3$ （HITEC)	TiO_2	0.1	NA	5.5	[82]
HITEC	TiO_2	0.5	NA	-1.4	[82]
HITEC	TiO_2	1.0	NA	-6.2	[82]
Li_2CO_3-K_2CO_3	Al_2O_3	1.0	NA	32.0	[103]
NaCl-KCl-Na_2CO_3	Al_2O_3	2.0	4.3	31.3	[104]
NaCl-KCl-NaF	Al_2O_3	1.0	246	186	[105]
NaCl-KCl-NaF	CuO	1.0	170	125	[105]
HITEC	Al_2O_3	2.0	12.1	5.8	[106]
HITEC	CuO	0.1	NA	5.6	[107]
HITEC	CuO	1.0	NA	3.4	[107]
HITEC	CuO	3.0	NA	1.7	[107]
HITEC	CuO	5.0	NA	-2.4	[107]

It is widely accepted that liquid molecules form a semi-solid layer on nanoparticle surfaces with a crystalline-like structure, behaving differently from normal liquids. Related experiments on eutectic molten salts based NePCMs have shown that such semi-solid layer can even grow into larger microstructures, potentially forming an interconnected network and enhancing thermal performance. Tiznobaik et al. [102] observed that silica nanoparticles of varying sizes (5-60 nm) in an eutectic molten salt Li_2CO_3-K_2CO_3, significantly increased the specific heat by about 25.0%, apparently independent of the size of the nanoparticles. SEM observations revealed needle-like structures formed by the molten salt near nanoparticle surfaces, as depicted in Fig. 14(a), which were unique to nanomaterials with enhanced specific heat. The backscattered electron micrograph image shows (Fig. 14(b)) that the brightness of the needle-like structure is significantly higher than that of the matrix molten salt, which suggests that the molar composition or the phase state may have changed there. The authors suggested that the surface charge-induced microstructural reorganisation was at the core of the specific heat capacity enhancement. The presence of hydroxyl groups on the surface of SiO_2 may partially dissociate into the negatively charged Si-O^- in the high-temperature molten salts, which attracts the cations in the molten salts. Due to the different charge densities of the different cations, they are adsorbed to different extents, leading to the formation of locally sub-stable phases, such as localized K^+-rich or Li^+-rich zones, or to the formation of new amorphous phases. This directed growth of chemical gradients is the main reason for the formation of needle-like structures. These structures have a larger specific surface area and special phase states that further enhance the specific heat capacity. In another study by the authors, they replaced silica with nano-alumina under identical conditions and observed similar chain-like nanostructures, leading to a comparable specific heat enhancement (32.0%) [103]. The conclusions suggest that nanoparticles themselves do not directly contribute to the specific heat enhancement. Instead, the formation of fractal tree-like long-range secondary nanostructures induced by nanoparticles as structure inducers is the main reason. El Far et al. [101] corroborated this by adding 0.03 wt% hydroxide to the nanofluid to disrupt nanostructures, resulting in a specific heat enhancement decrease from 19.0% to 9.0%.

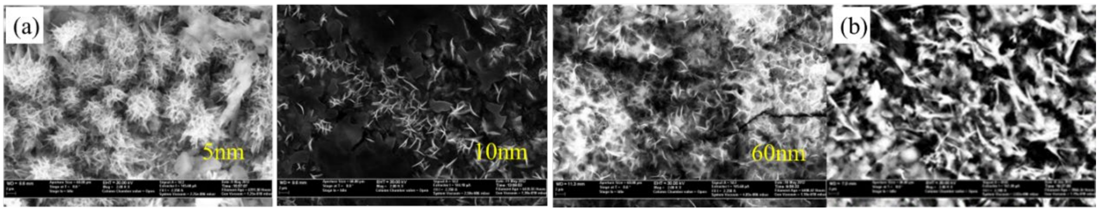

Fig. 14 (a) SEM images and (b) backscattered electron micrograph of NePCM [102]

The review indicates that nanoparticles with a high specific surface area tended to be more favourable for the growth of nanostructures, which in turn significantly increases the specific heat of NePCMs. Tao et al. [55] prepared composite PCMs using binary carbonate eutectic salt doped with carbon nanomaterials and found that graphene incorporation resulted in the highest specific heat enhancement, showing an 18.6% specific heat improvement with only 1.5 wt% of addition. It is speculated that SWCNTs are the most favorable for the enhancement of the specific heat capacity compared to MWCNTs and fullerene C60. This is due to the large specific surface area of graphene and SWCNT, which are 2013.3 and 1781.5 m^2/g, respectively, promoting the growth of nanolayers. Similarly, Wu et al. [105] observed that 1.0 wt% alumina nanoparticles increased the average specific heat of ternary eutectic molten salt NaCl-KCl-NaF by 2.46 and 1.86 times in solid and liquid states, respectively, whereas copper oxide nanoparticles at the same mass fraction led to increases of 1.70 and 1.25 times, respectively.

In addition, the influence of nanoparticle concentration is also significant. Aljaerani et al. [82] found that 0.1% TiO_2 increased the heat capacity of KNO_3-$NaNO_2$-$NaNO_3$ (HITEC) salt by 5.5%, but higher concentrations of 0.5% and 1.0% reduced it by 1.4% and 6.2%, respectively, due to the dispersion deterioration under high nanoparticle loads. Aljaerani et al. [107] reported specific heat enhancements of 5.6%, 3.4%, 1.7%, and -2.4% for HITEC molten salt doped with 0.1 wt%, 1.0 wt%, 3.0 wt%, and 5.0 wt% CuO nanoparticles, respectively. Xiao et al. [106] improved the thermal properties of HITEC salts by doping with alumina nanoparticles, achieving maximum enhancement rates of 12.1% and 5.8% in solid and liquid states at a nanoparticle concentration of 2.0 wt%.

In summary, there have been a number of studies that have highlighted the dependency of specific heat enhancement on nanostructure growth, nanoparticle type, concentration, and base PCM composition. However, the current mechanism is based on analyses and speculations on the microstructure, which is apparently not sufficient. Future research could further determine the chemical composition of the needle-like structures by energy dispersive spectrometer or X-ray photoelectron spectroscopy. In addition, the phonon contribution of the nanostructures needs to be quantified in conjunction with molecular dynamics simulations. It is also significant to further optimize the formation of needle-like structures by changing the surface conditions of the nanoparticles, e.g. regulating the density of -OH. Notably, the evolution of needle-like structures during long-term thermal cycling is also worth investigating.

3.3.2 Other PCM based NePCMs

Studies on the specific heat of NePCMs beyond molten salt bases are sparse. It is widely known that when the specific heat of the nanoparticles is lower than that of the base liquid, the nanofluid typically has a lower specific heat [108]. He et al. [109] observed that adding TiO_2 nanoparticles to paraffin decreased its specific heat, with reductions of 2.9% and 12.4% at 10 °C for 0.167 vol% and 1.130 vol% nanofluids, respectively, and 2.3% and 9.0% at 80 ℃. Kumar et al. [110] reported that copper oxide at 0.5, 1.0, and 3.0% mass fractions reduced the specific heat of paraffin by 2.7%, 5.2%, and 14.0%, respectively. Liu et al. [111] also found that the doping of Au nanoparticle with a specific heat of only 0.129 J/g K resulted in a decrease in specific heat for sorbitol based NePCMs.

Contrary effects were noted by Lu et al. [62], who found that Fe_3O_4 nanoparticles did not reduce the specific heat of paraffin, which is possibly due to the latent heat compensation during phase changes. Luo et al. [112] improved thermal storage performance of erythritol with nano titanium dioxide, showing variable specific heat enhancement depending on the nanoparticle fraction and the temperature. In general, the solid state showed a higher specific heat improvement than the liquid state. This is due to the fact that the ordered structure in the solid state is disrupted by the added nanoparticles, resulting in an increase in the number of interfaces and a further increase in the proportion of interfacial atoms. These atoms are in a sub-stable state with different vibrational modes and conformational entropy from those inside the crystal, and the increased vibrational freedom significantly increases the heat capacity. Apparently, the smaller the nanoparticles, the higher the relevant contribution. In the liquid state, where the material itself is already in a disordered state, this influence is negligibly small. On the contrary, the enhancement of the liquid specific heat is mainly influenced by the interfacial thermal resistance and the semi-solid layer mentioned earlier, and these interfacial effects are further weakened by the high degree of fluidity. The study by Aslfattahi et al [113], on the other hand, focused on the enhancement effect of specific heat at high temperatures. The experimental results showed that 0.3 wt% MXene enhanced the specific heat capacity of paraffin-based nanocomposites from 3.11 J/g K to 4.43 J/g K at 250 ℃, indicating an increase of 42.4%. It was suggested that this was mainly related to the increase in molecular vibration, rotation and translational motion at high temperatures, which led to an increase in the average energy of the molecules, thus storing more energy.

There may also be a material dependence to the change in specific heat. El-Sebaii et al. [114] found that different nanoparticles, such as nano-copper oxide and nano-alumina, had contrasting effects on nanofluid specific heat, as depicted in Fig. 15. Abdelrazik et al. [115] added GNPs and MWCNTs nanoparticles to pure paraffin and observed that PW/GNPs samples had higher specific heat than PW/MWCNTs samples, except for concentrations ≥1.0 wt%, where PW/GNPs exceeded liquid specific heat of pure PW. This was attributed to broader interactions between PW and GNPs and potential instabilities in nanocomposite PCM behavior, such as aggregation or bubble capture during preparation, leading to inconsistent composite responses [115], as depicted in Figs. 16 and 17.

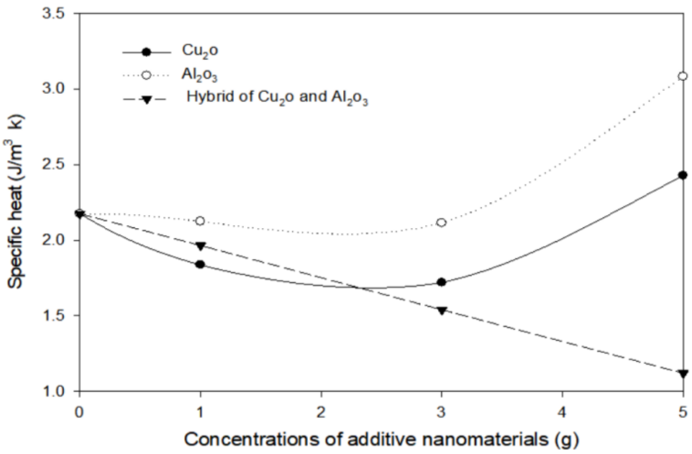

Fig. 15 Specific heat of paraffin with different concentrations of different nanomaterials [114]

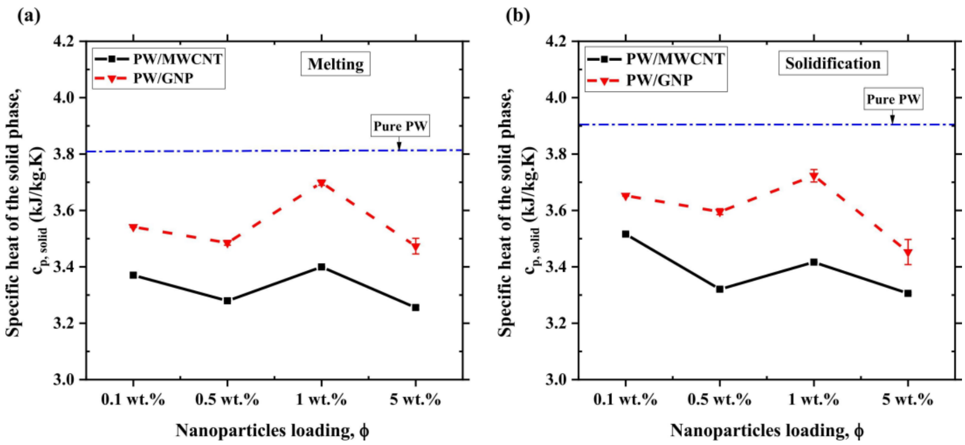

Fig. 16 Comparison of solid-state specific heat of NePCMs with different concentrations of nanoparticles [115]

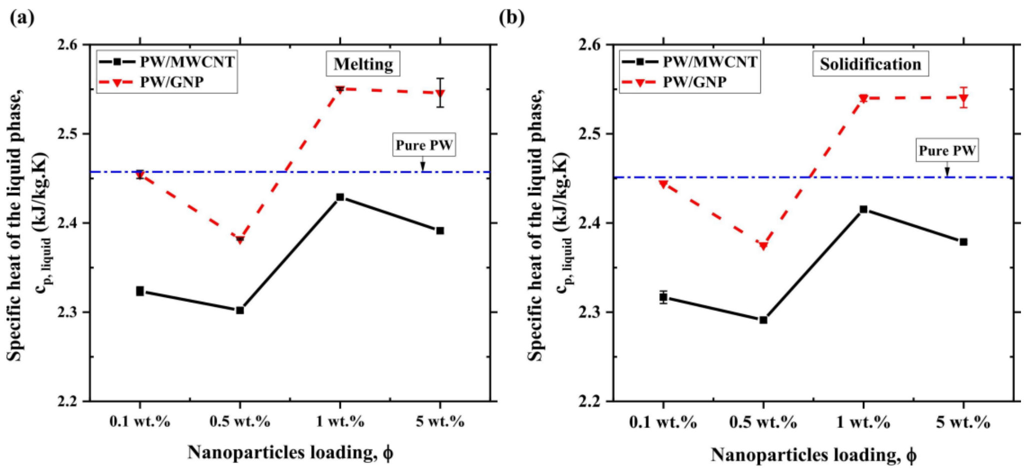

Fig. 17 Comparison of liquid-state specific heat of NePCMs with different concentrations of nanoparticles [115]

3.4 Summary in sensible heat

Sensible heat storage in PCMs involves the absorption or release of thermal energy through temperature changes in the solid or liquid phases. Recent studies have shown that by incorporating nanoparticles into PCMs to form NePCMs, the specific heat capacity can be significantly improved, enhancing the material's ability to store thermal energy. This enhancement is attributed to several mechanisms, including the high surface energy of nanoparticles which strengthens their interaction with surrounding molecules, the increasing interfacial thermal resistance caused by the large surface area of nanoparticles, and the formation of semi-solid layers around the nanoparticles that require additional energy to break down.

In eutectic molten salt-based NePCMs, the presence of nanostructures formed near nanoparticle surfaces appears to be a critical factor in the enhancement of specific heat. The type and concentration of nanoparticles also play crucial roles in determining the extent of specific heat enhancement. Studies have shown that low concentrations of nanoparticles yield the best results, while higher concentrations can lead to particle agglomeration and reduced dispersion quality, ultimately lowering the specific heat.

Beyond molten salts, research on other types of NePCMs, such as those based on paraffin, sorbitol, and erythritol, is more limited and presents contradictory results. In many cases, adding nanoparticles with lower intrinsic specific heat than the base fluid leads to an overall reduction in specific heat, as seen with TiO_2, CuO, and Al_2O_3 in paraffin-based nanofluids. However, some studies have reported positive effects, particularly when nanoparticles influence latent heat or interfacial energy.

Moreover, the compatibility of nanoparticles with the base PCM significantly affects the resulting thermal properties. The findings suggest that both physical and chemical interactions between nanoparticles and the base PCM need to be specifically considered to achieve consistent and effective thermal performance.

However, the results in various studies on sensible heat storage using NePCMs remain inconsistent, highlighting the complexity of nanoparticle-PCM interactions. Variations in experimental methods, nanoparticle dispersion techniques, and measurement conditions contribute to these discrepancies, emphasizing the need for further investigation and standardization. Future research should focus on the better understanding the formation and the evolution of nanostructures within NePCMs, as well as the optimization of nanoparticle selection and concentration to maximize thermal performance without compromising the stability of NePCMs.

4 Rheological property

4.1 Mass fraction and temperature

It is widely recognized that the effective dynamic viscosity of nanofluids increases with increasing of the mass fraction of nanoparticles and decreases with increasing of the temperature. Ho et al. [61] reported intensified friction between nanoparticles and the base liquid with an increase of the particle fraction and the viscosity. Srinivasan et al. [116], on the other hand, suggested that it was mainly due to fluid molecule stratification on nanoparticle surfaces, reducing the effective number of flowable fluid molecules. They also proposed that at high nanoparticle concentrations, the viscosity might decrease due to particle aggregation. He et al. [109] suggested that as temperature rose, nanoparticle Brownian motion was enhanced, weakening intermolecular attraction and decreasing viscosity. Asadi et al. [117] found that temperature increase energized nanofluid molecules, boosting molecular kinetic energy and intensifying atomic movement, which overcame the intermolecular adhesiveness and reduced the base fluid dynamic viscosity.

At higher concentrations, the viscosity of NePCM can be predicted using the Brinkman correlation equation [118]:

$$\mu_{\mathrm{NePCM}} = \mu_{\mathrm{PCM}}/(1-\varepsilon)^{2.5} \tag{14}$$

where μ_{NePCM}, μ_{PCM} and ε stand for viscosity of NePCM, viscosity of the base PCM and the weight fraction of nanoparticle, respectively.

Motahar et al. [119] studied the rheological properties of n-octadecane doped with 0.0~5.0 wt% titanium dioxide nanoparticles over 5~55 °C. It was found that Newtonian behavior at 1.0 wt% nanoparticle fraction and a transition to non-Newtonian occurred at 2.0 wt% and above. Similar results were obtained at higher nanoparticle mass fractions above 1.0 wt%, where a transition from shear-thinning behavior was observed [120]. Newtonian fluid behavior is marked by a linear relationship between shear rate and applied shear stress.

$$\tau = \mu \cdot \dot{\zeta} \tag{15}$$

where τ is the shear stress, μ is the viscosity coefficient, and ζ is the shear strain rate. The power law liquid model is commonly used to describe the characteristics of non-Newtonian fluids, and the characteristics of power law fluids are as follows:

$$\tau = K \cdot \zeta^n = K \cdot \zeta \cdot \zeta^{n-1} = \eta \cdot \zeta \tag{16}$$

where the apparent viscosity is defined as

$$\eta = K \cdot \zeta^{n-1} \tag{17}$$

K represents the dynamic viscosity, and η represents the power law index, reflecting the degree of closeness to Newtonian behavior. When η=1 and K=μ, the fluid is Newtonian. When η<1, it is a pseudoplastic fluid (shear-thinning behavior), and when η>1, the fluid is a dilatant fluid (shear-thickening behavior).

Zhuang et al. [121] investigated the rheological properties of n-octadecane nanofluids with copper oxide, aluminum oxide, and titanium dioxide nanoparticles at varying mass fractions. The results indicated all samples displayed pseudoplastic behavior, transitioning to Newtonian behavior beyond a critical shear rate where the viscosity became independent on the shear stress. This transition was attributed to the "de-aggregation" of nanoparticles under a high shear, leading to increased dispersion, reduced viscosity, and eventual Newtonian flow. The study concluded that shear-thinning behavior correlated with the nanoparticle aggregation. With higher mass fractions, larger critical shear rates were required for better dispersion, exhibiting higher stable apparent viscosities. Delgado et al. [122] noted that under static conditions, particles were randomly dispersed, but under increased shear, particles realigned into layers parallel to the flow direction, reducing interlayer friction and viscosity by decreasing the average inter-particle distance in the flow direction while increasing it perpendicular to the flow direction. This realignment facilitated easier movement and lower viscosity of the NePCMs.

4.2 Types of nanoparticles

The properties of nanoparticles, such as shape and size, have significant influence on the viscosity of NePCMs. For example, the effect of different carbon nano-additives on the viscosity of paraffin-based was explored by Yu et al. [123]. The results showed that the addition of short CNTs led to a dramatic deterioration in viscosity. With nanoparticles addition of 4.0 wt%, the viscosity increased by more than 140 times compared to the base solution. The authors concluded that short carbon nanotubes tended to form a high-density network structure, which significantly increased the flow resistance. The planar GNPs were the most effective in inhibiting the viscosity increase. Interestingly, the viscosity change of the GNPs samples did not vary monotonically with loading concentration. There existed a certain critical point beyond which the viscosity turned down. This was due to the two-dimensional planar structure of GNPs that might undergo the shear-induced alignment and the interlayer sliding under high loadings. Fan et al. [52] noted that 0.3 wt% CNTs in 1-hexadecanol at 80 °C increased viscosity by 115.0%, compared to 16.5% with GNPs. Therefore, the unique planar structure and shear response properties of GNPs are advantageous in practical applications.

Singh et al. [124] reported that doping with 0.1 vol%, 0.3 vol%, and 0.5 vol% of SiO_2 (10-20nm), Al_2O_3 (20nm), and MgO (35nm) increased paraffin viscosity by 66.6%-91.6%, 66.6%-88.9%, and 66.6%-87.5%, respectively. Harikrishnan et al. [125] found that 1.0 wt% TiO_2, ZnO, and CuO increased the viscosity of a MA-SA eutectic by 2.6%, 2.9%, and 3.7%, respectively, with CuO having a more significant negative impact due to the larger surface area of the rod-like structure.. Similar results were also seen in the study by Nithiyanantham et al. [126]. This indicated that smaller size and larger specific surface area resulted in more significant viscosity gains. However, a different conclusion was reached in the study by Fang et al. [127]. 5 wt% of GNS-30 (larger sized graphite nanosheets) increased the dynamic viscosity of pure eicosanes from 3.4 cP to 156.7 cP, which was more than a 40-fold increase, whereas the smaller sizes of GNS-60 and GNS-180 resulted in a lower increase in viscosity, which was 131.5 cP and 97.02 cP, respectively. They suggested that intensified particle interactions was the most likely cause but did not launch into an in-depth discussion.

4.3 Surface modification

Avid et al. [75] used octadecyltrimethoxysilane for the silanisation of MWCNTs, which enhanced the compatibility with the base solution paraffin and significantly improved the dispersion stability of the nanoparticles. In addition, the original MWCNT tended to agglomerate and form a network structure, which hindered the movement of paraffin molecules and increased the flow resistance of the system. The long chains of octadecyltrimethoxysilane connected MWCNT and paraffin through covalent bonding, which facilitated the directional alignment of the nanotubes, reduced the internal friction between the hydrocarbon chains, and inhibited the agglomeration phenomenon. Test results showed that the viscosity of the sample with 0.5 wt% and 1.0 wt% unmodified MWCNTs was 20 times and 80 times higher than that with Si-MWCNTs. The phenomenon described above is regarded as the "nano-lubrication" effect, which has also been seen in other studies [128, 129]. On the contrary, Noori et al. [130] observed that modified CuO surfaces with grafted organic layers increased the viscosity and the PCM stability.

Progress in nanoparticle synthesis and surface modification has improved nanoparticle-base fluid interactions, leading to a more predictable viscosity in NePCMs [131]. Dispersion methods such as ultrasonication and surfactant use have also aided in achieving uniform nanoparticle distribution and minimizing viscosity increases.

However, viscosity in NePCMs remains complex due to variability in nanoparticle characteristics. Increased viscosity can elevate pump power needs and reduce heat transfer efficiency. Long-term NePCM stability is also a concern, with potential nanoparticle aggregation affecting the viscosity. Comprehensive models capable of predicting NePCM viscosity under varying conditions are needed.

4.4 Influence on performance of NePCMs

The increase in nanoparticles generally enhances thermal conductivity, however, the increase in viscosity inhibits natural convection during the melting process, which in turn affects the performance of the TES system. Therefore, a trade-off needs to be made between enhanced thermal conductivity and reduced natural convection.

Taking the study by Das et al. [132] as an example, as shown in Fig. 18, most of the heat transfer processes can be categorized into similar three stages: in the initial stage mainly dominated by heat conduction, with time the upper part showing a buoyancy-driven natural convection mode and the lower part by heat conduction. At the same time, the shape of the melt front starts to change and asymmetric melting in the vertical plane appears. After a sufficiently long time, e.g., when t=7200, convection induced by the liquid-phase phase change material starts to dominate.

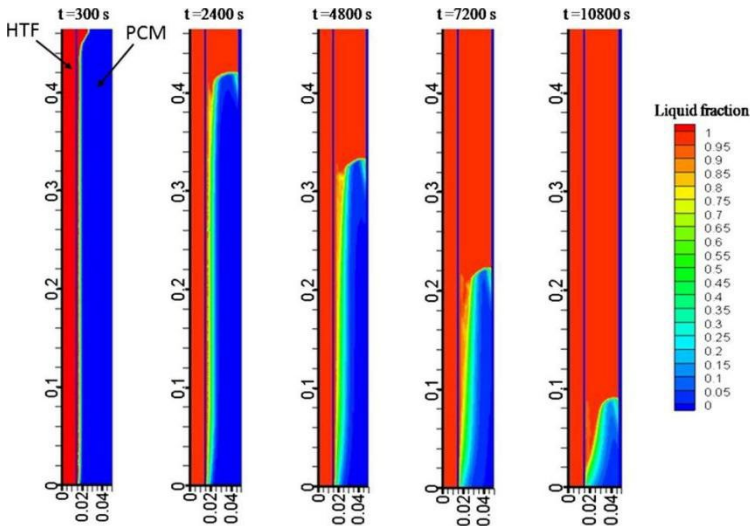

Fig.18 Plot of liquid fraction contours of pure PCM over time [132]

As shown in Fig. 19, they also simulated the effect of different shapes of carbon-based nanoparticles on the melting behavior of n-octane in a vertical latent heat thermal energy storage system. 1 vol% of spherical nanodiamond brought only 2.0% of thermal conductivity enhancement, which was nearly negated by 2.5% viscosity enhancement. Therefore, the advancement of its melting front was almost the same as that of pure PCM. In contrast, SWCNT and GnP at the same mass fraction resulted in 38% and 71.0% thermal conductivity enhancement, respectively, supporting the rapid expansion of the melting front. Alazwari et al. [133] numerically analyzed the thermal properties of nanoparticle doped mannitol in a vertical shell and tube LHTES device. The results showed that carbon-based nanomaterials significantly reduce the melting time due to their low density and high heat capacity. Similar results were found in Sun et al. [134].The continuous layered structure of nanographite was more advantageous in improving the melting behavior of PCMs than that of nano coconut shell charcoal with irregular stacking of carbon atoms.

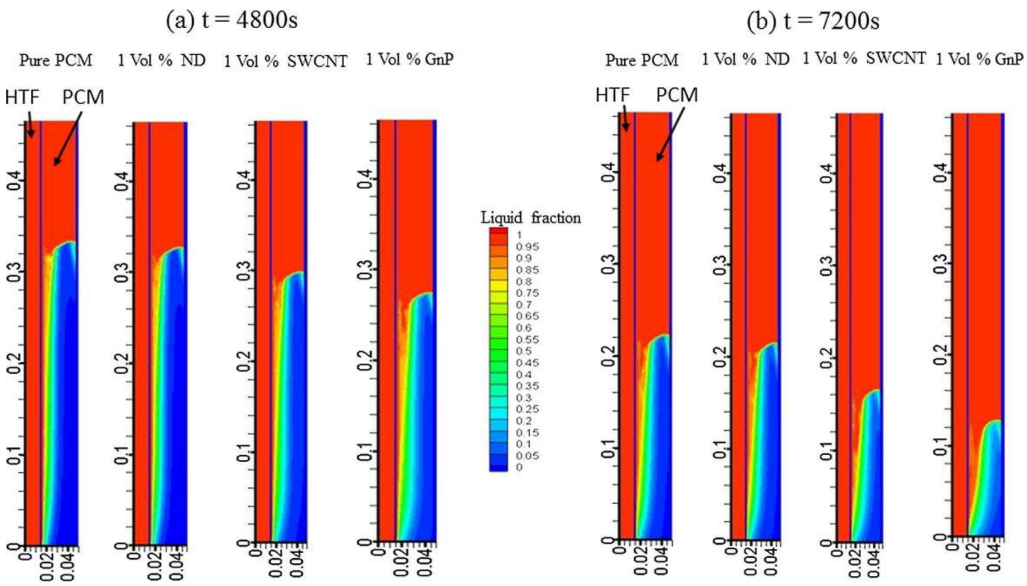

Fig. 19 Liquid fraction for different nanocomposites [132]

Fan et al. [135] experimentally investigated the melting of graphite nanosheets doped with 1-dodecanol in a spherical vessel. The results showed that 0.5 wt% NePCM reduced the melting time by 5 min compared to pure PCM, in contrast to 1.0 wt% NePCMs, which still prolonged the total melting time by about 11 min due to the more than 60-fold increase in dynamic viscosity, despite of increasing the thermal conductivity by more than 50%,. Bahiraei et al. [136] found that among three different carbon-based nanoparticles with mass fractions ranging from 2.5% to 10.0%, only 7.5 wt% and 10.0 wt% graphite-based PCMs enhanced the thermal performance of the TES system due to 620.0% and 1100.0% enhancement in thermal conductivity. Iachachene et al. [137] studied transient numerically the melting of NePCM embedded in trapezoidal cavities based on enthalpy-hole technique. The results showed that improved heat transfer performance could not be achieved when the increase in thermal conductivity was less than 80.0% compared to pure PCM.

However, Zeng et al. [138] found negligible natural convection in the 2.0 wt% NePCM sample by calculating the *Gr* value, which could not give an optimistic performance improvement for the TES system, despite of the fact that the sample had the largest thermal conduction enhancement. Li et al. found that 3.0.wt% CNT dramatically deteriorated the rheological properties of NePCM, and that the temperature of the TES system would increase by 5-10 ℃ due to the almost disappearing natural convection. In fact, natural convection should not be ignored, since heat conduction dominates only in the initial stages of melting. In addition, Dhaidan et al. [139] concluded that lower concentrations of nanoparticles also provided a higher energy storage capacity, more stable systems and lower costs.

Therefore, future studies should focus more on the selection of suitable nanoparticles in systems that will have low concentration loading. It is worth noting that there exists another important reason for accelerating the melting rate, the reduction of latent heat, especially at higher particle loadings. However, at present, researchers do not seem to be coupling this with the viscosity and the thermal conductivity.

Solid nanoparticles in the base PCM are known to increase the viscosity and increase the resistance of the pipeline flow process, thereby increasing the pipeline pumping power. Eq. (18) can be used to evaluate the pipeline pumping power (P) demand [140]:

$$P = 8L\mu\pi u^2 \quad (18)$$

where the viscosity (μ) and flow rate (u) of the fluid are taken into account. To determine u, the volumetric flow rate can be derived from reference [141], as shown in Eq. (19):

$$G = Q/\rho\Delta h_{\mathrm{t}} \quad (19)$$

where Q is the heat transfer capacity, ρ is the density, and Δh_{t} is the total heat capacity, including both latent and sensible heat.

In conjunction with Section 3, when nano-doping reduces the latent heat, the required pumping flow rate increases with the same heat load, which inevitably ends up increasing the pumping power consumption of the system. When nano-doping increases the latent heat, it offsets the harsh effects of increased viscosity and reduces the pumping power to some extent.

4.5 Summary in rheological property

The rheological properties of NePCMs are significantly influenced by nanoparticle mass fraction and temperature. It is widely recognized that the effective dynamic viscosity of nanofluids increases with higher nanoparticle concentrations but decreases as temperature rises. The increase in viscosity is attributed to intensified friction between nanoparticles and the base fluid, as well as fluid molecule stratification on nanoparticle surfaces. However, at high concentrations, particle aggregation may counterintuitively reduce the viscosity. Additionally, as temperature increases, enhanced Brownian motion of nanoparticles weakens intermolecular attraction, thereby decreasing the viscosity. To predict the viscosity at higher nanoparticle concentrations, the Brinkman correlation equation can be applied, which incorporates the weight fraction of nanoparticles and the viscosity of the base PCM.

At low nanoparticle concentrations (<1.0 wt%), NePCMs tend to exhibit Newtonian behavior. However, at higher concentrations, they transit to non-Newtonian behavior, showing shear-thinning characteristics. This behaviour is related to nanoparticle aggregation and depolymerisation behaviour and is commonly described by power-law models.

The type and morphology of nanoparticles also play a crucial role in determining the rheological properties of NePCMs. Carbon-based nanomaterials, such as CNTs and GNPs, significantly impact the viscosity. Similarly, rod-shaped nanoparticles induce more viscosity increases than spherical ones due to their structure.

Surface modification of nanoparticles further influences the viscosity by improving the dispersion stability. Surfactants and organic layers grafted onto nanoparticles can increase the viscosity while enhancing the stability. Methods like ultrasonication and surfactant addition have proven to be effective in achieving uniform nanoparticle distribution, though they complicate viscosity trends. Despite of these advancements, predicting the change of viscosity remains challenging due to the variability in nanoparticle characteristics, long-term stability concerns, and the potential for aggregation.

The trade-off between enhanced thermal conductivity and increased viscosity becomes particularly important when evaluating the performance of TES systems. While nanoparticles generally improve the thermal conductivity, the resulting viscosity increase suppresses natural convection during melting, affecting the heat transfer efficiency. Researchers have observed that lower nanoparticle concentrations (<2.5 wt%) optimize TES system performance by balancing thermal conductivity, viscosity, and latent heat reductions. Additionally, the pipeline pumping power required for NePCMs flow can be evaluated using equations that account for the viscosity, the flow rate, and the heat transfer capacity.

Future research could focus on optimizing the nanoparticle selection and loading to achieve balanced improvements in thermal conductivity, viscosity, and latent heat. Comprehensive models capable of coupling these factors under varying conditions are needed to advance NePCMs applications in TES systems. Additionally, the impact of surfactants and surface modifications on the viscosity requires further investigations to stabilize nanodispersions without excessive viscosity penalties.

5 Thermal conductivity

Thermal energy storage and release rates of PCMs are linked to the thermal conductivity. Nanoparticle inclusion enhances solid-phase conduction, melting process and liquid-phase convection. This section will analyze and summarize the mechanisms behind thermal conductivity enhancement in both solid and liquid states.

5.1 Solid state

Heat transfer mechanisms in solids primarily involve conduction, with phonon theory explaining the thermal conduction in non-metallic PCMs. As shown in Fig. 20, The lattice of any material can be considered as a system of atoms and springs, the interaction forces between atoms are approximated as elastic forces. When heated, the vibration will deviate from the equilibrium position. Phonons, as quantized lattice vibrations, transfer thermal energy from heated surface atoms to adjacent atoms, facilitating heat diffusion through the crystal lattice, which forms the temperature gradient. Fig. 21 shows the generation of a temperature gradient under the phonon diffusion mechanism, in which high-energy phonons are generated at the hot end and gradually lose their energy during the transport.

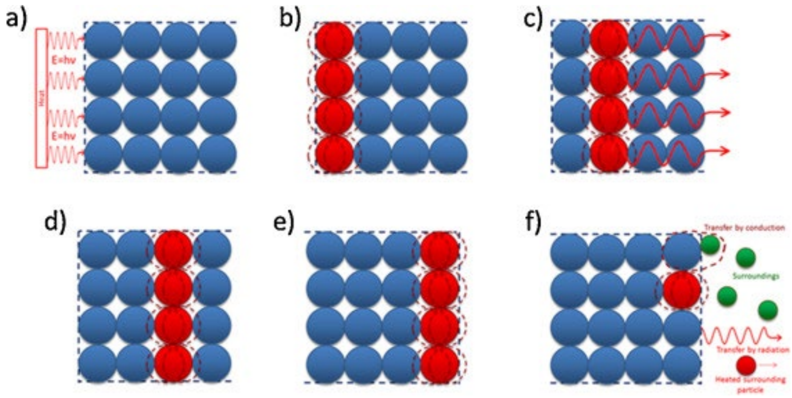

Fig. 20 Schematic diagram of phonon theory [142]

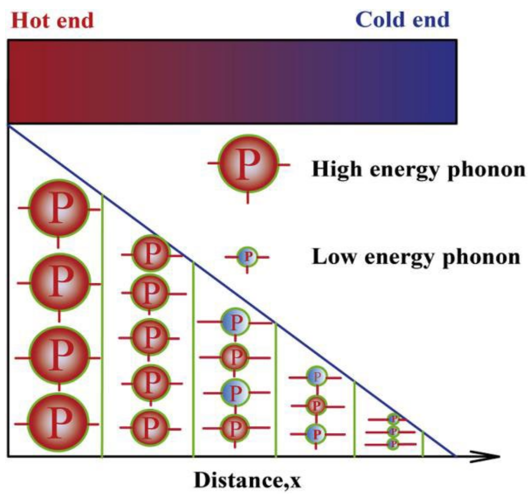

Fig. 21 Temperature curve with length and phonon energy diagram [143]

Thermal conductivity depends on the efficiency of phonon transport. Higher thermal conductivity is achieved when phonon propagation is unimpeded, while scattering mechanisms degrade it. In an ideal defect-free lattice where phonons do not interact, thermal conductivity could theoretically be infinite. However, in practice, phonon transfer involves inevitable scattering events that alter direction, momentum, or energy, thereby reducing heat transfer efficiency.

Based on kinetic theory and treating phonons as pseudo-particles, the Debye model provides the following expression for thermal conductivity:

$$\lambda = \int c_{\mathrm{v}}(w) \cdot v(w) \cdot l(w)/3 \tag{20}$$

where c_{v} is the constant-volume specific heat capacity, v is the phonon group velocity, and l is the phonon mean free path. The heat capacity c_{p} increases with temperature (proportional to T^3 at low temperatures) and approaches a constant value at high temperatures, approximately three times the gas constant. Phonon velocity v depends on elastic stiffness and mass density [144], while the mean free path l represents the average distance traveled between scattering events; longer l corresponds to higher thermal conductivity. There are numerous factors that affect the l, for example, temperature rise increases phonon excitation and collision probability, leading to shorter l.

Major scattering mechanisms include phonon-phonon, phonon-defect, and phonon-interface interactions, as illustrated in Fig. 22 [145]. Enhancing thermal conductivity in nanocomposites relies on forming a continuous thermal conduction network that minimizes phonon scattering.

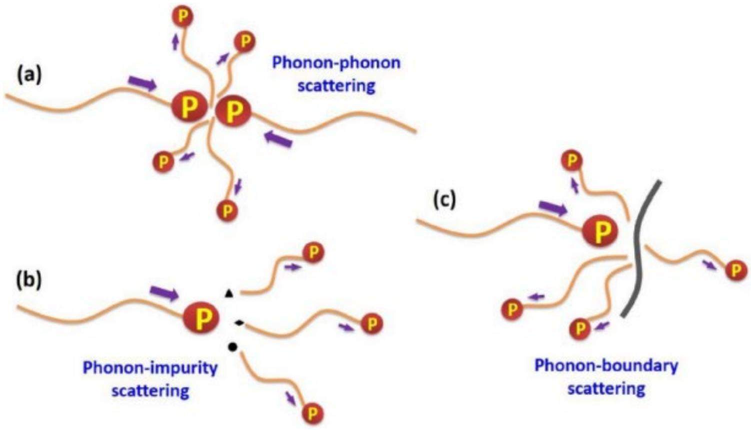

Fig. 22 Three phonon scattering mechanisms [145]

Due to the presence of multiple frequencies and normal modes, it is impossible for all atoms to vibrate in a harmonic form. The actual lattice follows anharmonic vibrations, which inevitably leads to phonon-phonon scattering. A typical model is Umklapp scattering, which can be described as the eventual merger of two waves initially moving to the right to form a wave moving to the left, called "Umklapp" in German. The process is only consistent with the conservation of energy, rather than the conservation of momentum.

Phonon-defect scattering results from lattice defects such as point defects, dislocations, and impurities, which reduce thermal conductivity by shortening the phonon mean free path through reflection, diffraction, or refraction. Kim et al. [146] demonstrated that high-temperature treatment can convert short, defective CNTs into long, straight, highly crystalline tubes, significantly enhancing their thermal conductivity. Their results showed that 7.0 wt% phenolic resin combined with highly crystalline CNTs increased thermal conductivity from 250 W m^{-1} K^{-1} to 393 W m^{-1} K^{-1}. Similar improvements via filler crystallinity enhancement have been reported elsewhere [147-149].

Phonon propagation in finite crystalline domains also leads to phonon-boundary scattering. In composites, additional phonon scattering occurs at filler-matrix interfaces due to acoustic impedance mismatches [150]. Enhancing nanomaterial compatibility with the PCM matrix helps mitigate such scattering and improves the thermal conductivity of NePCM.

Forming strong covalent bonds at the interface through surface functionalization has been proven to improve interfacial heat transfer. Avid et al. [75] found 1.0 wt% modified MWCNTs enhanced paraffin PCM conductivity by up to 30.0%. This is because the long carbon chains of the silane coupling agent octadecyltrimethoxy silane are covalently bonded on the surface of the MWCNTs, connecting the Si-MWCNTs and the paraffin matrix, and reducing the interfacial thermal resistance. Similarly, Ganguli et al. [151] performed surface silanization of exfoliated graphite flakes, and the thermal conductivity of the epoxy resin at 20 wt% loading increased by a factor of 28, compared to a factor of 19 before modification. Yuan et al. [152] quantified interfacial bonding interaction energies in NePCMs using molecular dynamics simulations. The interaction energy was calculated as:

$$E_{\mathrm{Interaction}} = E_{\mathrm{total}} - E_{\mathrm{nanoparticle}} - E_{\mathrm{PCM}} \quad (21)$$

where E_{total} represents the total energy of the NePCM, and $E_{\mathrm{nanoparticle}}$ and P_{EPCM} represent the energies of the isolated nanoparticle and PCM components, respectively. As shown in Fig. 23, functionalization of graphene with ethyl, hydroxyl, and carboxyl groups significantly enhanced interfacial interaction energies, with the effect increasing at higher functional group coverage. The improved interfacial integration effectively restricted molecular chain slippage in the composite system [153]. Additionally, phonon vibrational compatibility between contacting materials plays a key role. Greater overlap of vibrational modes leads to lower interfacial thermal resistance and stronger heat transfer. Based on phonon vibration power spectrum analysis [154], the ethyl-functionalized sample exhibited the highest mode overlap, resulting in a 59.8% improvement in thermal conductivity at 10% coverage, compared to 31.5% and 36.7% for hydroxyl- and carboxyl-modified cases, respectively.

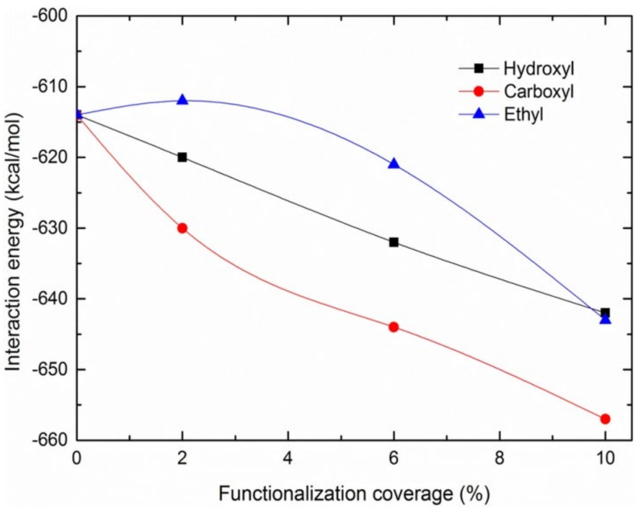

Fig. 23 Plot of interaction energies with different functional group coverages [152]

However, some researchers [155, 156] noticed that surface functionalization, while improving dispersion and matrix coupling, could damage the filler's surface structure, create new defect locations and reduce its intrinsic thermal conductivity, which suggested that the surface modification wasn't preferable in this case. A trade-off may exist between enhancing interfacial thermal conductivity and preserving the intrinsic thermal conductivity of the filler. Gulotty et al. [157] observed that functionalizing CNTs with carboxyl groups introduced structural defects such as broken sp^2 bonds, sp^3 covalent bonds, and C-H sites, which limited thermal conductivity improvement despite strengthening CNT-matrix bonding. Liu et al. [158] similarly noted that surface modification can degrade the material’s intrinsic thermal performance. Functionalization, while beneficial for interfacial adhesion, introduces phonon-scattering defects, highlighting the challenge of optimizing functionalization degree (e.g., coverage) to minimize such losses. Future work should focus on defect control, cost-effective processing, and synergistic optimization of multiple performance metrics.

Additionally, longer and larger fillers are expected to exhibit higher thermal conductivity due to reduced interfacial density. Park et al. [159] demonstrated this effect by showing that 10 wt% short-MWCNT/epoxy composites had a thermal conductivity of 0.35 W m^{-1} K^{-1}, whereas 2.0 wt% and 6.38 wt% long-MWCNT composites achieved 0.9 W m^{-1} K^{-1} and 2.6 W m^{-1} K^{-1}, respectively. Xiang et al. [160] found 15 μm exfoliated graphite nanoplatelets were more effective than 1 μm in enhancing the thermal conductivity of paraffin composites. Reducing xGNPs size from 15 μm to 1 μm could lower the thermal conductivity by 90.0%. Luo et al. [161] simulated that elongated graphene flakes improved the interfacial heat transport by exciting long-wavelength phonons. Fang et al. [127] utilized ball milling to control the size of graphene nanosheets (GNS), and the ball milling time was inversely proportional to the finished size. The results showed that the samples after 30 mins' ball milling had the largest size and 258% enhancement in thermal conductivity was induced at 5.0 wt% loading compared to the eicosanoidal solution, while the enhancement of the samples treated for 60 min and 109 min was 180% and 109%, respectively. Debelak et al. [162] noted the thermal conductivity of large-flake system increased linearly with the graphite content, while that of the systems with smaller flakes increased at a slightly slower rate with the increase of graphite content.

Many other studies have focused on the shape of nanoparticles. The high specific surface area of spherical fillers resulted in more interfaces compared to planar fillers and did not seem to be an excellent option for improving the thermal conductivity [163, 164]. Planar nanomaterials like GNPs [165, 166] reduced the interfacial thermal resistance and enhanced the thermal conductivity more effectively than other nanomaterials. Fan et al. [167] found 5.0 wt% GNPs increased the thermal conductivity by 164.0%. Fan et al. [52] reported that 3.0 wt% GNPs enhanced the thermal conductivity of solid PCM composite by 170.0%, surpassing composite with CNTs at 31.1%. Prado et al. [168] found 1.0 wt% GNPs increased the thermal conductivity by 24.0%, compared to 3.0% for MgO nanoparticles. He et al. [169] reported that GNPs were superior for enhancing thermal conductivity of MA, which could improve the thermal conductivity by 176.3% with 3.0 wt% loading. This was the largest enhancement compared to 47.3% by MWCNTs and 44.01% by nano-graphite (NG).

In addition, there are relevant reports on the ability of hybrid nanoparticles to enhance heat transfer beyond single nanocomposites. Hayat et al. [73] reported hybrid nanocomposites had superior thermal performance, achieving peak thermal conductivity with 1.0 wt% GNPs+MWCNTs. Bharathiraja et al. developed materials with graphene nanosheets/nano-SiO_2 [170] and MWCNTs/nano-SiO_2 [54], which significantly outperformed single nanoparticles in thermal conductivity. Sathishkumar et al. [171] added MWCNT and nano-boron nitride to paraffin, increasing conductivity from 0.18 $W{\cdot}m^{-1}{\cdot}K^{-1}$ to 0.31 $W{\cdot}m^{-1}{\cdot}K^{-1}$. Ultrasonication and stirring were found to facilitate the heat transfer by creating a soft interface between the hybrid nanoparticles in the PCM. Arshad et al. [172] analyzed the thermal conductivity enhancement by titanium dioxide nanoparticles in RT-35HC coupled with MWCNT, GO, reduced graphene oxide, and GNP (Fig. 24). It was claimed that the three-dimensional matrix structure formed in the NePCMs improved the heat transfer in all directions. Chen et al. [173] prepared a composite PCM with GO and CNTs in paraffin, and explained that the increasing thermal conductivity was due to high conductivity channels formed by CNTs between the GO skeleton.

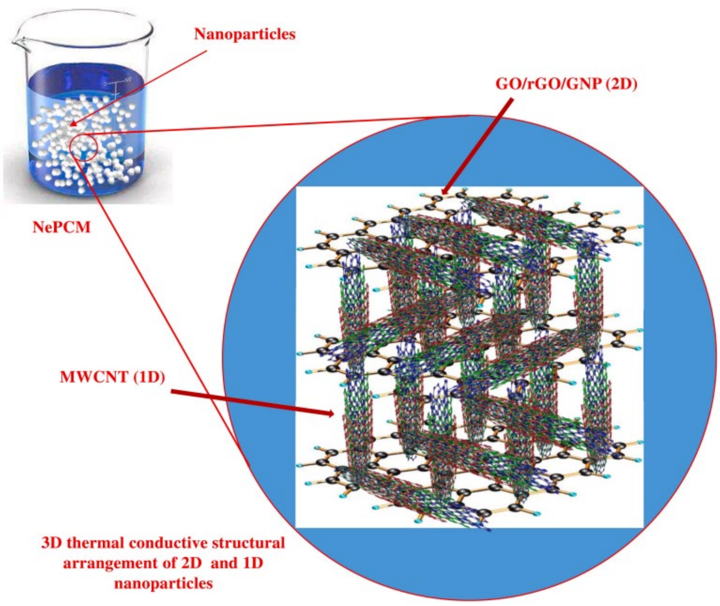

Fig. 24 Schematic diagram of three-dimensional thermal conductive arrangement of the NePCM with hybrid carbon additives [172]

5.2 Liquid state

As temperature increases, the matrix molecules' vibration intensifies, leading to the breakdown of PCM's solid structure and a transition to liquid state. Tong et al. [174] observed a thermal conductivity increase of 4.9%, 14.0%, and 17.4% in Zn-ZnO/paraffin with 0.01, 0.03, and 0.05 vol%, respectively, compared to the base paraffin. They attributed this to the change of the micro-movement between nanoparticles and the base fluid via Brownian forces, which enhanced the energy transfer and thermal conductivity. However, based on the kinetic theory, Evans et al. [175] reasoned to obtain an equation for the contribution of Brownian motion to the thermal conductivity when the fluid and particles move synchronously:

$$k_B = D_B c_p \tag{22}$$

where D_B is the diffusion coefficient of nanoparticles and c_p is the fluid specific heat capacity. Numerical calculations demonstrated that the thermal conductivity contribution of Brownian motion was less than 1.0% of the thermal conductivity of the base fluid, which was negligible. In addition, molecular dynamics simulations were done to investigate the thermal conductivity of nanoparticles with different wettability. The simulation results were in high agreement with the effective medium theory, which further verified that the negligible contribution of Brownian motion. Finally, it was inferred that the anomalous enhancement of thermal conductivity observed in the experiments might originate from the particle aggregation, although no further discussions were provided. Keblinski et al. [68] then calculated the particle diffusion time ($\tau_D \approx 2\times10^{-7}$ s) to be much larger than the thermal diffusion time ($\tau_H \approx 4\times10^{-10}$ s) by means of the Stokes-Einstein formula, which also demonstrated that the Brownian motion contribution to the direct heat transfer was negligible.

Researchers proposed that strong adsorption of nanoparticles led to a semi-solid layer with crystal-like morphology at the liquid-solid interface, differing from typical liquids. This layer, resembling the order of a crystal solid, served as a thermal bridge, enhancing heat transfer compared to the liquid. This layer was anticipated to increase thermal conductivity, with thicker layers leading to greater enhancement [98, 176, 177]. Zhao et al. [178] simulated the interface of silica nanoparticles with octadecane using molecular dynamics methods, observing a thermal conductivity increase from 0.142 $W\cdot m^{-1}\cdot K^{-1}$ to 0.268 $W\cdot m^{-1}\cdot K^{-1}$ as silica thickness increased from 0 to 15.0 Å. The authors suggested that the increased thickness of the nanolayer made the molecules more tightly arranged, and their high density and ordered structure reduced the phonon scattering and ensured the continuity of the heat conduction path. Conversely, Xue et al. [67], using molecular dynamics simulation, found no significant impact of liquid atom layer on thermal transport properties. Even when the wettable liquid was highly confined between solids, there was no significant change in its thermal conductivity. In addition, it was experimentally assumed that the layering thickness required to obtain achieve the theoretical thermal conductivity increase was 3 nm, whereas the simulation results showed that the ordering in the liquid layer extended only 1 nm. Its atomic vibrations remain short-range correlated and are unable to form long-range phonon propagation. In contrast, semi-solid layer may scatter phonons, disrupting heat transfer and reducing thermal conductivity.

Linking thermal conductivity enhancement to the aggregation behavior of the filler appears to be a promising approach. Researchers have associated improvements in thermal conductivity with either direct or fluid-mediated filler clustering effects, as illustrated in Fig. 25. For instance, Arshad et al. [179] studied titanium dioxide nanoparticles in RT-35HC and found that at 0.5 wt%, the particles were dispersed independently with a low thermal interface resistance, slightly enhancing the heat flow and thermal conductivity. At 0.5-1.0 wt%, intermolecular interactions increased, forming local clusters that improved heat transfer paths. Further concentration increases to 1.0-2.0 wt% facilitated a complete heat conduction network, significantly enhancing thermal conductivity. Gao et al. [180] observed that nano-aluminum oxide particles aggregated locally within the hexadecane crystal structure during freezing, forming rod-like clusters that were crucial for increasing thermal conductivity. During solidification, internal stress changes pushed nanoparticles towards grain boundaries, increasing the contact area between particles, reducing percolated nanoparticle network resistance, and enhancing thermal conductivity [181].

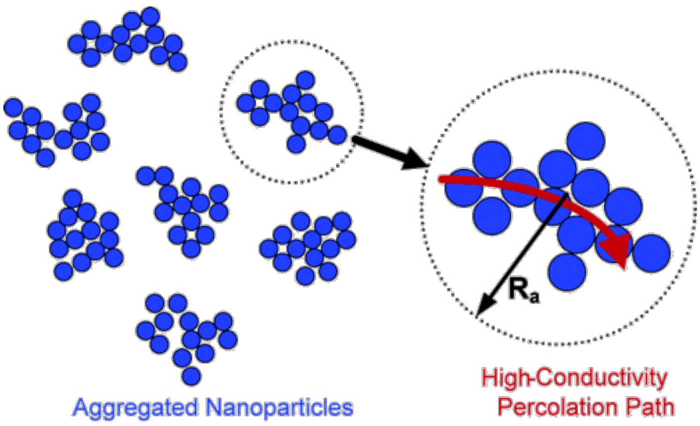

Fig. 25 Schematic diagram of clustering effect [69]

Keblinski et al. [68] introduced the theory of ballistic heat transfer into nanofluid research for the first time, and proposed the concept of "liquid-layer-mediated ballistic heat transfer" to explain the anomalous enhancement of thermal conductivity at low volume fractions. Specifically, when the size of the nanoparticles was much smaller than the phonon mean free range, it could be assumed that the phonons had almost no scattering within the particles but propagated in a ballistic mode, as shown in Fig. 26(a), where there was almost no energy dissipation and the heat could instantaneously across the whole particle. By determining the heat flow autocorrelation function through molecular dynamics simulations, the authors also found that when the phonons propagated to the solid-liquid interface, some of the phonons were reflected and oscillatingly decayed, while some of the phonons were transmitted into the liquid and monotonically decayed, as shown in Fig. 26(b).

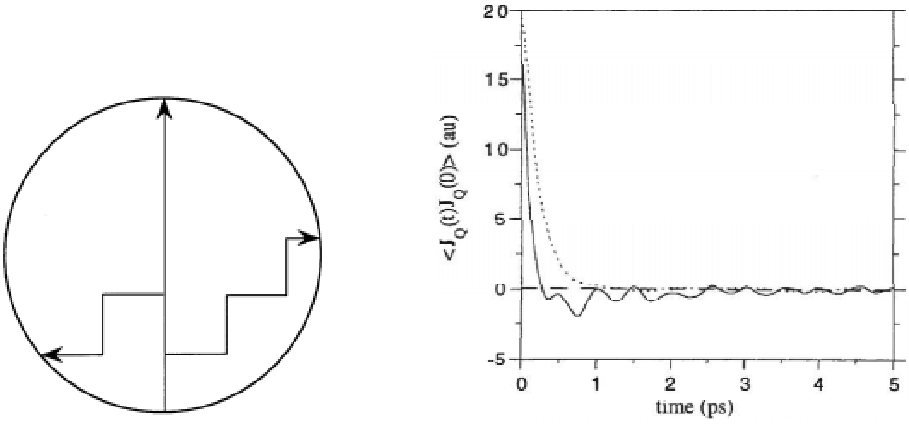

Fig. 26(a) Schematic diagram of ballistic and diffusive phonon transport mechanisms in a solid particle and (b) Plot of heat flow autocorrelation function for liquid (dashed line) and particles (solid line) [68]

Liquid-mediated aggregation means that closely spaced localized clusters can be formed when nanoparticles are dynamically approached through a very thin liquid layer. As shown in Fig. 27, even at low volume fractions, the distance between particle surfaces is still at the nanometre level, e.g., 5 nm particles at 5 wt% at an average spacing equal to approximately 2 nm, while local regions may be closer. In addition, although Brownian motion cannot explain the thermal conductivity enhancement alone, it can however contribute in facilitating the dynamic proximity of particles. When the particle spacing is sufficiently small, ballistic effects may penetrate the liquid layer and extend to neighboring particles, enabling coherent heat transfer between particles. The effective heat transfer network thus forms speaks far beyond macroscopic theoretical predictions. However, the specific decay mechanism of ballistic phonons in the liquid layer is still unclear and further studies need to be carried out. In addition, the quantification of the contribution of ballistic heat transfer to the macroscopic thermal conductivity still needs to be experimentally verified.

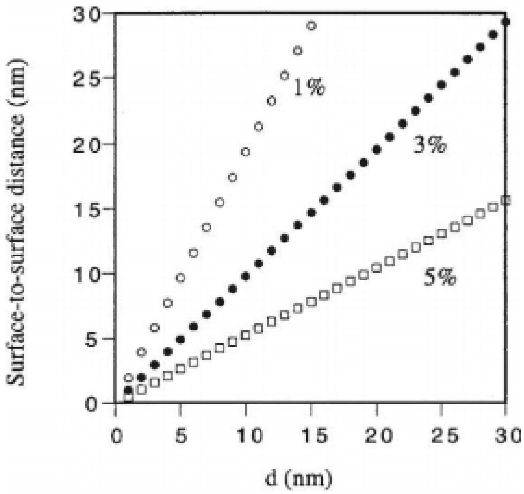

Fig. 27 Plot of mean surface distance between particles as a function of particle diameter *d* [68]

In the context of liquid PCM thermal conductivity, the impact of viscous forces need to be considered. Fan et al. [135] suggested that in liquid conditions, the presence of nano-enhancers created a trade-off between enhanced thermal conductivity and increased viscosity, influencing the melting rate. Higher viscosity could impair natural convection and the squeezing effect in melting regions, resulting in thicker melting layers that impeded the heat conduction. Dhaidan et al. [182] studied nanofluids with nano-CuO particles and found that increased nanoparticle concentration could raise dynamic viscosity and led to aggregation and sedimentation, limiting heat transfer enhancement. Jesumathy et al. [183] observed that paraffin with 10.0 wt% copper oxide loadings increased thermal conductivity by 7.8%, while dynamic viscosity rose by 30.0%. Another study [61] reported that at 30 °C, thermal conductivity of paraffin with 5.0 wt% and 10.0 wt% aluminum oxide nanoparticles increased by over 2.0% and 6.0%, respectively, with dynamic viscosity increasing by nearly 20.0% and 28.0%, which was significantly higher than the thermal conductivity enhancement. At 60 °C, thermal conductivity enhancement rose by 17.0%, possibly due to the enhanced Brownian motion and the reduced viscosity in the base fluid.

Interfacial thermal resistance at the solid-liquid interface is significant. Wang et al. [184] modified carbon fibers (CF) with hydroxides to form M-CF and dispersed them in PA, reducing interface thermal resistance. At 70 °C, 0.5 wt% M-CF/PA increased the thermal conductivity by 305.6%, compared to 7.3% for CF/PA. Li et al. [185] acidified CNTs and grafted them with octanol (C8), tetradecanol (C14), and SA (C18), as shown in Fig. 28, resulting in shorter, less entangled nanotubes. Thermal conductivity of pure paraffin is 0.2312 $W \cdot m^{-1} \cdot K^{-1}$, while that of 1.0% carbon nanotube-doped paraffin was measured as 0.4272 $W \cdot m^{-1} \cdot K^{-1}$. Composite PCMs of CNTs-C8/paraffin, CNTs-C14/paraffin, and CNTs-C18/paraffin had thermal conductivities of 0.5355 $W \cdot m^{-1} \cdot K^{-1}$, 0.6326 $W \cdot m^{-1} \cdot K^{-1}$, and 0.6454 $W \cdot m^{-1} \cdot K^{-1}$, respectively. Rebrovic et al. [186] noted that longer nanotubes interacted more with themselves and less with the fluid, hindering dispersion in the base liquid and reducing the thermal conductivity of the nanofluid.

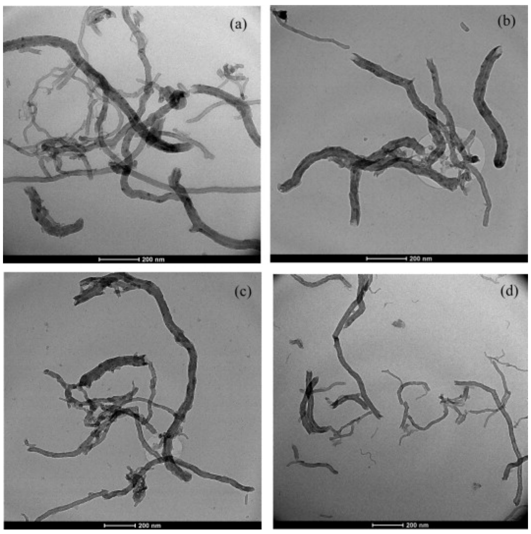

Fig. 28 Transmission electron microscopy images of (a) PCNTs, (b) CNT-C8, (c) CNT-C14 and (d) CNT-C18 [185]

Despite of the multitude of mechanisms that have been proposed, there remains a degree of contention. Nevertheless, these proposed mechanisms offer substantial heuristic value in elucidating the factors contributing to the enhanced thermal conductivity observed in NePCMs.

5.3 Comparison between solid and liquid states

Solid-state structures generally exhibit a superior thermal conductivity, with a marked enhancement in the solid phase. Thermal conductivity plummets as the structure transitions into a disordered liquid state. Kumar et al. [187] dispersed 0.5-2.0 wt% nano-oxidized copper particles in paraffin and determined the thermal conductivity through experiments and theory, finding higher conductivity and enhancement rates in the solid phase. Maximum enhancement was observed at 2.0 wt%, with a 172.7% increase in the solid phase versus 8.9% in the liquid. Bahiraei et al. [136] reported significant thermal conductivity increases in solid NePCM samples with added nano-fiber, GNP, and graphite, with negligible changes in the liquid phase. Masoumi et al. [188] noted a 15.0% and 7.0% increase in the thermal conductivity of SA with 0.39 wt% TiO_2 in the solid and liquid phases, respectively. Harish et al. [189] showed that the thermal conductivity enhancement of solid lauric acid at 2.0 vol% SWCNH filling was 37.0%, which was significantly higher than that of the liquid state at 11.0%. They suggested that thermal conductivity can be significantly improved in the solid state by crystal confinement and interfacial thermal resistance modulation. Specifically, during the curing process, nanomaterials are easily captured and trapped within the grain boundaries, creating "nano-enriched" areas. In addition, the internal stresses generated by crystal growth reduced the contact thermal resistance between nanoparticles, which synergistically increased the thermal conductivity of the solid NePCM. During the melting process, the internal stress releases, the contact area was reduced and the interfacial thermal resistance increased, resulting in a weaker enhancement of thermal conductivity. The authors also used an effective medium theory model to fit the experimental data and obtained an interfacial thermal resistance of 1.3×10^{-8} m^2 K W^{-1} in the liquid state, while it was an order of magnitude lower at 1×10^{-9} m^2 K W^{-1} in the solid state, further validating the improvement of interfacial contact by grain boundary stress. Ghossein et al. [190] measured the effective thermal conductivity of CuO/eicosane NePCM under different solidification conditions, with samples in an oven showing the highest thermal conductivity and those in an ice bath the lowest. This indicated that longer solidification times promoted the trapping of nanoparticles through grain boundaries, leading to the formation of larger and richer grains and a reduction in the number of grain boundaries, which in turn reduced the phonon scattering caused by the grain boundaries, and significantly improved the thermal conductivity of the solid NePCM structure.

However, researchers need to further investigate the dynamic behavior of the nanoparticle-matrix interface during long-term phase transition cycles, such as stress release and contact reconstruction, which can be observed with the aid of microimaging to observe the distribution of nanoparticles and interface evolution during the phase transition.

Experimental studies have noted a sharp increase in thermal conductivity near the melting point in the solid state, followed by a significant decrease upon melting. Wang et al. [191] modified carbon nanotubes (TCNTs) with potassium hydroxide to prepare hydroxyl-modified CNTs in a PA composite, with thermal conductivity results depicted in Fig. 29 (a). The authors attributed this to accelerated molecular vibrations in the solid state, which were disrupted by the disorder in the liquid state, causing a thermal conductivity drop. Motahar et al. [119] observed the thermal conductivity in TiO_2-n-octadecane composites across solid (5-25°C), phase change (25-30°C), and liquid (30-55°C) regions, as shown in Fig. 29 (b). Thermal conductivity was influenced by the nanoparticle mass fraction and the temperature, particularly in the phase change region due to the crystal structure instability. Nourani et al. [192] observed similar phenomena near 55°C and 35°C, potentially linked to solid-solid phase changes and latent heat absorption. PCMs with high thermal conductivity near phase change temperatures were deemed suitable for TES applications [188, 193, 194].

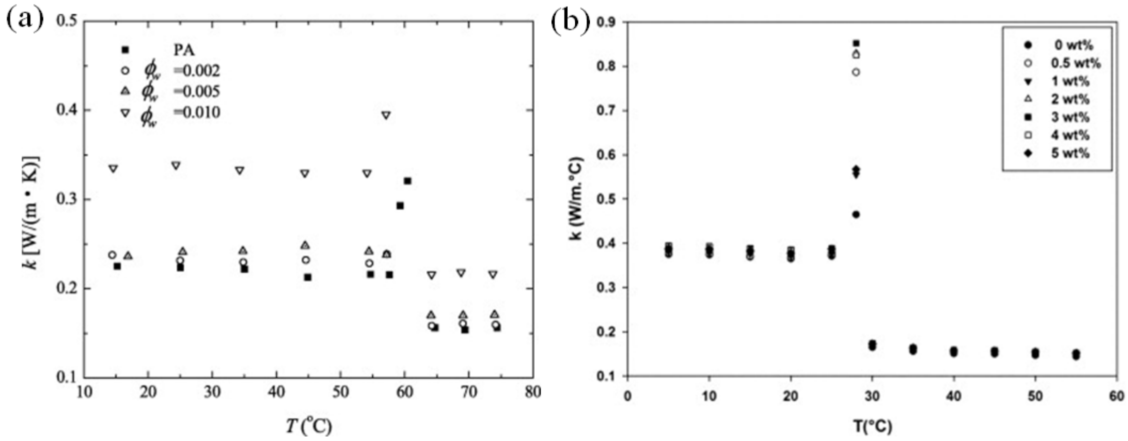

Fig. 29 Thermal conductivity of (a) PA and PA/TCNTs at different temperatures [191] and (b) n-octadecane/TiO2 at different loads and temperatures [119]

Temperature dependence of thermal conductivity enhancement was also investigated. He et al. [169] measured the thermal conductivity enhancement in 3.0 wt% GNPs, MWCNTs, and NG-doped paraffin, as shown in Fig.30(a). Thermal conductivity remained stable below 50 °C and above 60 °C but exhibited a stepwise decrease within the phase change range, attributed to the disruption of the solid-state percolation network. Qian et al. [195] observed a slight increase in the thermal conductivity of PEG with 2.0%-10.0% SWCNTs under solid conditions, as depicted in Fig. 30 (b), but noted a significant decrease within the phase change range. Krishna et al. [196] reported analogous findings in their experimental and theoretical studies.

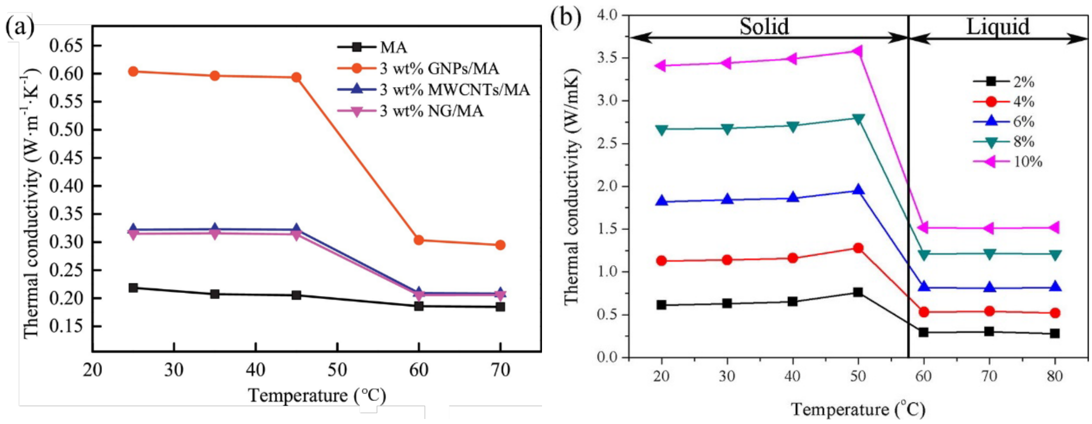

Fig. 30 Thermal conductivity of (a)MA, 3.0 wt% GNPs/MA, 3.0 wt% MWCNTs/MA and 3.0 wt% NG/MA [169] and (b) PEG/SWCNTs nanocomposites as a function of temperature [195]

Some existing studies also prove an increase in thermal conductivity in the liquid state over the solid state. Wu et al. [197] prepared Cu/paraffin composite PCMs, finding that 2.0 wt% Cu increased the thermal conductivity by 14.2% in the solid state and 18.1% in the liquid state. Jegadheeswaran et al. observed that Cu doping at 0.5 wt%, 1.0 wt%, 2.0 wt%, and 3.0 wt% increased the thermal conductivity of paraffin by 7.0%, 14.0%, 24.0%, and 30.5% in the solid state, and 8.0%, 15.0%, 28.0%, and 31.5% in the liquid state, respectively. Gao et al. [198] used non-equilibrium molecular dynamics simulation to calculate the thermal conductivity of PA/graphene composite PCMs. It was found that doping with 1.0, 3.0, and 5.0 wt% graphene increased solid-state thermal conductivity by 13.2%, 32.7%, and 36.4%, and liquid-state thermal conductivity by 12.2%, 34.6%, and 40.4%, respectively. Fan et al. [52] noted that after melting, the thermal conductivity enhancement of hexadecanol base/CNT composite PCM increased from 31.1% to 40.6%, which suggested that microscale transport phenomena like Brownian motion and thermophoresis might be responsible. Wang et al. [184] proposed that during PCM melting, CFs tended to cluster, reducing the effective nanoparticle load and thus the solid-state thermal conductivity and enhancement rate of NePCMs. In the liquid state, fiber clusters were more likely to disperse, particularly at low loads, leading to higher thermal conductivity enhancement rates than in the solid state.

5.4 Summary in thermal conductivity

The domain of NePCMs has witnessed significant advancements that have substantially broadened our capacity to modulate thermal conductivity, a pivotal parameter for efficient heat transfer within TES applications. The incorporation of nanoparticles into PCMs has been identified as a robust approach to enhance thermal conductivity. Empirical evidence has indicated that nanoparticles can facilitate additional heat flow pathways, consequently increasing the thermal conductivity of the PCM. This enhancement is especially advantageous in applications requiring rapid heat absorption, release or dissipation, where conventional PCMs fall short due to their inherently low thermal conductivity. The utilization of hybrid nanoparticles has demonstrated particular efficacy in further increasing thermal conductivity due to their synergistic interactions among the constituent nanoparticles. In parallel, the refinement of predictive models for NePCM thermal conductivity has progressed significantly, offering a more accurate and reliable foundation for the rational design and optimization of NePCMs. Despite of these advancements, several challenges hinder optimization of the thermal conductivity in NePCMs. A predominant issue is the variability in reported thermal conductivity enhancements attributed to nanoparticle incorporation, which reflects the complex interaction between nanoparticle characteristics and the base PCM. These interactions are not yet fully understood and may be influenced by factors including particle dispersion quality, the formation of agglomerates that disrupt heat flow, or variations in interfacial phonon scattering dynamics. Additionally, discrepancies in measurement methodologies across studies may amplify observed inconsistencies. Additionally, the introduction of nanoparticles leads to an increase in viscosity of the resulting NePCMs, which can counteract the benefits of improved thermal conductivity by hindering the fluid flow. Another critical concern lies in the long-term stability of the enhanced thermal conductivity; nanoparticles may undergo sedimentation or aggregation over time, potentially degrading the heat transfer performance. Addressing these challenges will require a more in-depth exploration of the underlying mechanisms governing nanoparticle-PCM interactions, along with the development of standardized experimental protocols for nanoparticle dispersion. By systematically elucidating these mechanisms and refining experimental frameworks, future studies can bridge gaps in reproducibility and realize the full potential of NePCMs in TES systems, enabling more efficient and sustainable energy efficiency utilization.

6 Applications, economic and environmental analysis

NePCMs, with their enhanced thermal characteristics, are increasingly integrated into TES systems and play an important role in various applications. Extensive literature have highlighted their contributions to applications such as battery thermal management systems [199-201], building thermal management systems [202, 203], solar collectors [204-206], refrigeration and heat pumps [207, 208], photovoltaic thermal systems [209, 210], among others. For achieving a more energy-efficient and environmentally friendly future, it is crucial to consider the economic and environmental impacts and challenges associated with designing PCM-integrated systems. These factors are equally important for ensuring scalability and long-term sustainability.

Economic analysis is essential for making sound investment decisions and commercializing the technology. There are several factors that need to be considered and evaluated:

(1) Material cost: This involves material cost, production cost and long-term durability. The selected PCM should tend to come from biobased or renewable sources that are not only relatively inexpensive, but also can be easily broken down or recycled for reprocessing, reducing energy consumption and environmental burdens [211]. Common nanoparticles, e.g., carbon-based, are expensive. Some studies have proposed that nanoparticles can be prepared from waste materials, as shown in Table 5.

(2) Energy saving: NePCM's enhanced thermal performance can further improve system efficiency. Islam et al [224] integrated NePCMs with a photovoltaic thermal (PVT) systems and launched an outdoor experimental study in Malaysia. The results showed that the PVT-NePCMs system was able to achieve an overall energy efficiency and exergy efficiency of 85% and 12%, respectively, which were significantly higher than the conventional system. Al-Kayiem and Lin [225] found that integrated TES filled with Cu nanoparticle-based NePCMs can increase the efficiency of flat-plate solar collectors by 8.4%. Krishna et al. [226] investigated the performance improvement of Al_2O_3-based NePCMs for electronic component cooling and showed that NePCMs significantly improved the heat pipe cooling module by

reducing the evaporator temperature by approximately 25.75% and saving 53% of the fan power consumption. By quantifying energy efficiency improvements and clarifying the energy saving potential and energy efficiency, it is possible to estimate the economic advantage in terms of energy costs over the life cycle of the system.

Table 5 Sources and properties of waste materials-derived nanofillers

Nanoparticle	Recyclable waste	Properties of nanoparticle	Ref.
Carbon nanoparticles	Waste plastic bags	Layer spacing 0.417-0.423 nm	[212]
SiC	Electronic waste CDs	Particle size 40-90nm Spherical structure	[213]
$A1_2O_3$	Ceramic waste	Particle size < 50 nm	[214]
SiO_2	Waste silicon sludge	Particle size 20–45 nm, Average pore size 10.52 nm, Specific surface area 430.9 m^2/g	[215]
TiO_2	Paper mill waste water	Particle size 10-15 nm Irregular circular aggregated structures	[216]
Fe_3O_4	Steel pickling waste liquor	Particle size 20-50 nm	[217]
$CaCO_3$	Eggshell	Particle size < 10 nm Surface area 44 m^2/g	[218]
$Ca_3(PO_4)_2$	Egg, mussel and quahog shells	Particle size 20 µm	[219]
CuO	Synthetic wastewater representing	Particle size 5–50 nm	[220]
Ag	Co-fired ceramic waste	Particle size 100 nm	[221]
Cellulose nanocrystals	Banknote production waste	Particle size 70 nm	[222]
Expanded glass aggregate (EGA)	Glass waste product	Particle size 0.25-4mm Particle density 310-540 kg/m^3	[223]

(3) Payback period: It needs to weigh the initial outlay of deploying a NePCMs system against the long-term advantages that can be realized. Cheaper ingredients,

higher energy efficiency and longer service life can result in a positive return on investment, making these technologies economically viable and attractive. A techno-economic analysis on a PVT system with integrated paraffin/SiC nanoparticles was performed by Al-Waeli et al. [227]. The results showed that the system could achieve a maximum thermal efficiency of 72.0% with a payback period of 4.4-5.3 years, which was found to be economically promising. Yousefi et al. [228] innovatively used recycled EGA as a PCM carrier to prepare NePCMs, which was integrated with cement mortar. Considering the use of this material in family-sized houses in Australia, the results showed that the maximum indoor temperature fluctuation in the building did not exceed 5 ℃, which resulted in a significant reduction in cooling and heating energy consumption. Additionally, the payback period for the production and initial installation costs of EGA-PCM was 25 years, which made this technology economically viable considering that most buildings had a service life of between 50-100 years. Rajamony et al. [229] integrated and experimentally investigated MWCNTs reinforced hydrated salt-based NePCMs with a PVT. The results showed that the cost of generating 1 kilowatt (kW) of electricity for the PVT system was 0.38 MYR, while that of the PVT-NePCM was 0.36 MYR, resulting in a significant reduction in electricity costs. In addition, the payback periods for the PVT and PVT-NePCMs systems were 60 and 55 months, respectively.

The assessment of the environment can also be discussed in several ways:

(1) Origin and processing of materials: On one hand, materials obtained from the natural environment are economical, but there is a need to avoid problems such as depletion of resources and destruction of habitats caused by over-exploitation. On the other hand, the production and processing of NePCMs may involve the generation of pollutants, and needs to be given for proper disposal and recycling for waste utilization.

(2) Energy saving and emission reduction: Energy efficiency of the system can be improved through energy savings and improved performance of the energy system,

as already mentioned in section 6.1, thus further reducing dependence on fossil fuels and greenhouse gas emissions. For example, Al Qattan [230] conducted a performance simulation of an Egyptian residential building with integrated nanoporous materials. The results showed that the NePCMs case saved more than 22.0% of energy consumption in electrical operation and helped to reduce the carbon dioxide content of the air in the apartment building by 18.0% compared to conventional buildings.

(3) Durability and long-term sustainability: It relates to the ability of a material to maintain the effectiveness of its original function over a longer operational period. Firstly, it is necessary to ensure that NePCMs does not degrade or deteriorate under continuous hot and cold cycles, especially in high temperature applications. In addition, the changes in nanoparticle distribution during prolonged operation need to be evaluated to overcome large-scale deposition and positional migration. In fact, this part of the work is relatively lacking at present, and most of the studies assume a uniform nanoparticle distribution under a continuous cycle. More in-depth studies of multi-cycle simulations considering changes in nanoparticle deposition effects, migration, degradation, etc. are needed in the future.

7 Conclusions, challenges and future research directions

An exhaustive examination of the preparation techniques, thermal capacity, viscosity, and thermal conductivity of NePCMs elucidates the achievements and challenges within this field. Drawing from a thorough review, the following conclusions are presented:

(1) The two-step preparation methodology for NePCMs offers enhanced control over nanoparticle characteristics and flexibility in material selection. This approach, favored for its industrial scalability, encounters difficulties in achieving homogeneous nanoparticle dispersion and maintaining the stability of the PCM matrix. In contrast, the one-step method, which integrates nanoparticle synthesis

with NePCMs preparation, offers less control over nanoparticle properties.

(2) The thermal capacity of NePCMs is markedly influenced by the incorporation of nanoparticles, typically leading to a reduction in latent heat. However, certain studies have reported an increase in latent heat, ascribed to augmented molecular interactions. The mechanisms underlying these enhancements warrant further exploration.

(3) Viscosity, a critical parameter affecting heat transfer efficiency and system operation, is generally increased due to the addition of nanoparticles. This poses challenges in terms of increased pump power requirements. Optimizing nanoparticle selection and dispersion methods to balance thermal performance with fluid flow dynamics is a pressing issue.

(4) The enhancement of thermal conductivity in NePCMs, a paramount objective in their development, has demonstrated promising outcomes. However, the temperature dependence of this enhancement is intricate and necessitates further research for a comprehensive understanding of the underlying mechanisms. While thermal conductivity has been significantly improved with nanoparticle incorporation, the variability in reported results and the impact on viscosity and long-term stability continue to be areas of concern.

Although research on NePCMs has made certain progress, there are still many unresolved issues and challenges that deserve further study.

(1) Ensuring that nanoparticles are uniformly dispersed and remain stable within PCMs over time is vital for maintaining consistent thermal performance. Nanoparticle aggregation, which can reduce the effective thermal conductivity and latent heat storage, poses a significant challenge. Strategies to prevent or mitigate aggregation are necessary to maintain the enhanced thermophysical properties of NePCMs. A critical challenge is ensuring the consistency and reproducibility of NePCM properties across different batches and over time, which is essential for reliable performance in real-world applications. Long-term

stability studies are needed to understand the behavior of NePCMs under repeated thermal cycling and over extended periods.

(2) Unraveling the intricate relationship between nanoparticle properties and the thermal behavior of PCMs is a key challenge. The phenomenon of nanoparticles increasing PCM latent heat requires further in-depth investigation.

(3) Enhancing the thermal conductivity of NePCMs typically necessitates increasing the concentration of nanoparticles, which may adversely affect latent heat storage and viscosity. A significant challenge is to identify methods for achieving thermal conductivity improvements at lower nanoparticle concentrations or to discover mechanisms for latent heat compensation and viscosity reduction. It is crucial to balance the enhancement of thermal properties with the increase in viscosity due to nanoparticle addition. Future research should focus on optimizing nanoparticle properties to maximize thermal performance while minimizing other critical characteristics such as the viscosity.

(4) Although hybrid nanomaterials have demonstrated potential in optimizing thermal conductivity, rigorous research on their synergistic effects is lacking. Future studies could benefit from exploring the hybrid arrangement and distribution of nanomaterials to minimize interfacial thermal resistance.

(5) The predominant methodologies for the fabrication of NePCMs are currently confined to laboratory scales. Advancing these techniques to facilitate industrial-scale production is important. It is crucial to explore and establish scalable production methodologies that preserve the uniformity and quality of NePCMs requisite for industrial applications. Additionally, comprehensive cost-benefit analyses should be undertaken to ascertain the economic feasibility of NePCMs for widespread implementation.

CRediT authorship contribution statement

Jiaxuan Li: Investigation, Writing-original draft. Songping Mo: Conceptualization, Funding acquisition, Project administration, Supervision, Writing-review & editing.

Lisi Jia: Writing-review & editing. Yanping Du: Writing-review & editing. Ying Chen: Resources.

Declaration of competing interest

The authors declare that they have no known competing financial interests or personal relationships that could have appeared to influence the work reported in this paper.

Data availability

No data was used for the research described in the article.

Acknowledgements

This work was supported by the National Natural Science Foundation of China [grant number 51976040].

References

[1] Kalapala L, Devanuri J K. Influence of operational and design parameters on the performance of a PCM based heat exchanger for thermal energy storage - A review. J Energy Storage 2018;20:497-519. https://doi.org/10.1016/j.est.2018.10.024.

[2] Mishra D K, Bhowmik C, Bhowmik S, Pandey K M. Property-enhanced paraffin-based composite phase change material for thermal energy storage: a review. Environ Sci Pollut R 2022;29:43556-87. https://doi.org/10.1007/s11356-022-19929-x.

[3] Al-Yasiri Q, Szabó M. Paraffin as a phase change material to improve building performance: An overview of applications and thermal conductivity enhancement techniques. Renew Energy Environ Sustain 2021;6:38. https://doi.org/10.1051/rees/2021040.

[4] Al-Ahmed A, Mazumder M A J, Salhi B, Sari A, Afzaal M, Al-Sulaiman F A. Effects of carbon-based fillers on thermal properties of fatty acids and their eutectics as phase change materials used for thermal energy storage: A Review. J Energy Storage 2021;35:102329. https://doi.org/10.1016/j.est.2021.102329.

[5] Wong-Pinto L S, Milian Y, Ushak S. Progress on use of nanoparticles in salt hydrates as phase change materials. Renew Sust Energ Rev 2020;122:109727. https://doi.org/10.1016/j.rser.2020.109727.

[6] Tony M A. Recent frontiers in solar energy storage via nanoparticles enhanced phase change materials: Succinct review on basics, applications, and their environmental aspects. Energy Storage 2021;3:e238. https://doi.org/10.1002/est2.238.

[7] Goel V, Dwivedi A, Kumar R, Kumar R, Pandey A K, Chopra K, Tyagi V V. PCM-assisted energy storage systems for solar-thermal applications: Review of the associated problems and their mitigation strategies. J Energy Storage 2023;69:107912. https://doi.org/10.1016/j.est.2023.107912.

[8] Wang X N, Li W G, Luo Z Y, Wang K J, Shah S P. A critical review on phase change materials (PCM) for sustainable and energy efficient building: Design, characteristic, performance and application. Energ Buildings 2022;260:111923. https://doi.org/10.1016/j.enbuild.2022.111923.

[9] Williams J D, Peterson G P. A review of thermal property enhancements of low-temperature nano-enhanced phase change materials. Nanomaterials-Basel 2021;11:2578. https://doi.org/10.3390/nano11102578.

[10] Nie B J, Palacios A, Zou B Y, Liu J X, Zhang T T, Li Y R. Review on phase change materials for cold thermal energy storage applications. Renew Sust Energ Rev 2020;134:110340. https://doi.org/10.1016/j.rser.2020.110340.

[11] Rajamony R K, Samykano M. Applications of nano-enhanced phase change materials in textiles, in: Z. Said, A.K. Pandey, editors. Nano Enhanced Phase Change Materials: Preparation, Properties and Applications, Singapore: Springer Nature Singapore; 2023, p. 201-22

[12] Jebasingh B E, Arasu A V. A comprehensive review on latent heat and thermal conductivity of nanoparticle dispersed phase change material for low-temperature applications. Energy Storage Mater 2020;24:52-74. https://doi.org/10.1016/j.ensm.2019.07.031.

[13] Barthwal M, Dhar A, Powar S. Effect of nanomaterial inclusion in phase change materials for improving the thermal performance of heat storage: A review. Acs Appl Energ Mater 2021;4:7462-80. https://doi.org/10.1021/acsaem.1c01268.

[14] Shah K W. A review on enhancement of phase change materials - A nanomaterials perspective. Energ Buildings 2018;175:57-68. https://doi.org/10.1016/j.enbuild.2018.06.043.

[15] Yang L, Huang J N, Zhou F J. Thermophysical properties and applications of nano-enhanced PCMs: An update review. Energ Convers Manage 2020;214:112876. https://doi.org/10.1016/j.enconman.2020.112876.

[16] Shin D, Banerjee D. Enhancement of specific heat capacity of high-temperature silica-nanofluids synthesized in alkali chloride salt eutectics for solar thermal-energy storage applications. Int J Heat Mass Tran 2011;54:1064-70. https://doi.org/10.1016/j.ijheatmasstransfer.2010.11.017.

[17] Porgar S, Oztop H F, Salehfekr S. A comprehensive review on thermal conductivity and viscosity of nanofluids and their application in heat exchangers. J Mol Liq 2023;386:122213. https://doi.org/10.1016/j.molliq.2023.122213.

[18] Manikanta J E, Nikhare C, Gurajala N K, Ambhore N, Mohan R R. A Review on hybrid nanofluids: preparation methods, thermo physical properties and applications. Iranian Journal of Science and Technology, Transactions of Mechanical Engineering 2024;49:67-79. https://doi.org/10.1007/s40997-024-00772-z.

[19] Asadi A, Aberoumand S, Moradikazerouni A, Pourfattah F, Zyla G, Estellé P, Mahian O, Wongwises S, Nguyen H M, Arabkoohsar A. Recent advances in preparation methods and thermophysical properties of oil-based nanofluids: A state-of-the-art review. Powder Technology 2019;352:209-26. https://doi.org/10.1016/j.powtec.2019.04.054.

[20] Abdullah A, Chowdhury A R, Yang Y C, Vasquez H, Moore H J, Parsons J G, Lozano K, Gutierrez J J, Martirosyan K S, Uddin M J. Tailoring the viscosity of water and ethylene glycol based TiO_2 nanofluids. J Mol Liq 2020;297:111982. https://doi.org/10.1016/j.molliq.2019.111982.

[21] Fan L W, Khodadadi J M. Thermal conductivity enhancement of phase change materials for thermal energy storage: A review. Renew Sust Energ Rev 2011;15:24-46. https://doi.org/10.1016/j.rser.2010.08.007.

[22] Choure B K, Alam T, Kumar R. A review on heat transfer enhancement techniques for PCM based thermal energy storage system. J Energy Storage 2023;72:108161. https://doi.org/10.1016/j.est.2023.108161.

[23] Kant K, Biwole P H, Shamseddine I, Tlaiji G, Pennec F, Fardoun F. Recent advances in thermophysical properties enhancement of phase change materials for thermal energy storage. Sol Energ Mat Sol C 2021;231:111309. https://doi.org/10.1016/j.solmat.2021.111309.

[24] Cheng P, Chen X, Gao H Y, Zhang X W, Tang Z D, Li A, Wang G. Different dimensional nanoadditives for thermal conductivity enhancement of phase change materials: Fundamentals and applications. Nano Energy 2021;85:105948. https://doi.org/10.1016/j.nanoen.2021.105948.

[25] Li S Y, Yan T, Pan W G. Two-dimensional nanosheets enhanced phase-change materials for thermal management applications. Cell Rep Phys Sci 2024;5:102046. https://doi.org/10.1016/j.xcrp.2024.102046.

[26] Tariq S L, Ali H M, Akram M A, Janjua M M, Ahmadlouydarab M. Nanoparticles enhanced phase change materials (NePCMs)-A recent review. Appl Therm Eng 2020;176:115305. https://doi.org/10.1016/j.applthermaleng.2020.115305.

[27] Sayyar M, Weerasiri R R, Soroushian P, Lu J. Experimental and numerical study of shape-stable phase-change nanocomposite toward energy-efficient building constructions. Energ Buildings 2014;75:249-55. https://doi.org/10.1016/j.enbuild.2014.02.018.

[28] Putra N, Amin M, Kosasih E A, Luanto R A, Abdullah N A. Characterization of the thermal stability of RT 22 HC/graphene using a thermal cycle method based on thermoelectric methods. Appl Therm Eng 2017;124:62-70. https://doi.org/10.1016/j.applthermaleng.2017.06.009.

[29] Liu X, Tie J, Wang Z Y, Xia Y T, Wang C A, Tie S N. Improved thermal conductivity and stability of Na_2SO_3•$10H_2O$ PCMs system by incorporation of Al/C hybrid nanoparticles. J Mater Res Technol 2021;12:982-8. https://doi.org/10.1016/j.jmrt.2021.02.096.

[30] Harikrishnan S, Magesh S, Kalaiselvam S. Preparation and thermal energy storage behaviour of stearic acid-TiO_2 nanofluids as a phase change material for solar heating systems. Thermochim Acta 2013;565:137-45. https://doi.org/10.1016/j.tca.2013.05.001.

[31] Prabhu B, ValanArasu A. Stability analysis of TiO_2-Ag nanocomposite particles dispersed paraffin wax as energy storage material for solar thermal systems. Renew Energ 2020;152:358-67. https://doi.org/10.1016/j.renene.2020.01.043.

[32] Xiao J B, Huang J, Zhu P P, Wang C H, Li X X. Preparation, characterization and thermal properties of binary nitrate salts/expanded graphite as composite phase change material. Thermochim Acta 2014;587:52-8. https://doi.org/10.1016/j.tca.2014.04.021.

[33] Deepak C N, Behura A K. Thermophysical characterization and reliability analysis of binary composite nano doping on stearic acid-acetamide eutectic PCM. Mater Today Sustain 2024;26:100804. https://doi.org/10.1016/j.mtsust.2024.100804.

[34] Mandal S K, Kumar S, Singh P K, Mishra S K, Bishwakarma H, Choudhry N P, Nayak R K, Das A K. Performance investigation of CuO-paraffin wax nanocomposite in solar water heater during night. Thermochim Acta 2019;671:36-42. https://doi.org/10.1016/j.tca.2018.11.003.

[35] Salyan S, Suresh S. Multi-walled carbon nanotube laden with D-Mannitol as phase change material: Characterization and experimental investigation. Adv Powder Technol 2018;29:3183-91. https://doi.org/10.1016/j.apt.2018.08.021.

[36] Singh D K, Suresh S, Singh H, Rose B A J, Tassou S, Anantharaman N. Myo-inositol based nano-PCM for solar thermal energy storage. Appl Therm Eng 2017;110:564-72. https://doi.org/10.1016/j.applthermaleng.2016.08.202.

[37] Vigneshwaran P, Shaik S, Suresh S, Abbas M, Saleel C A, Cuce E. Solar salt with carbon nanotubes as a potential phase change material for high-temperature applications: Investigations on thermal properties and chemical stability. Acs Omega 2023;8:17563-72. https://doi.org/10.1021/acsomega.2c07571.

[38] Taurozzi J S, Hackley V A, Wiesner M R. Preparation of nanoparticle dispersions from powdered material using ultrasonic disruption. Natl Inst Stan 2012;1200:1200-2. https://doi.org/10.6028/nist.Sp.1200-2.

[39] Jegadheeswaran S, Sundaramahalingam A. Experimental investigations of the effect of ultrasonic waves on the thermal performance of nanoparticles embedded phase change material. Int J Thermophys 2023;44:8. https://doi.org/10.1007/s10765-022-03123-9.

[40] Shahsavar A, Moradi M H, Arici M, Shamim T. An in-depth study of the effect of ultrasonic field on the melting characteristics of pure and nano-enhanced PCMs using thermal and digital imagery. J Energy Storage 2024;78:110054. https://doi.org/10.1016/j.est.2023.110054.

[41] Li H X, Zhuang Y J, Feng J C. Multi-scale experimental analysis on the coupled effects of ultrasonic field and magnetic field on the melting and energy storage performances for hybrid nano-enhanced phase change materials. J Energy Storage 2024;84:110801. https://doi.org/10.1016/j.est.2024.110801.

[42] Shen S, Tan S, Wu S, Guo C, Liang J, Yang Q, Xu G, Deng J. The effects of modified carbon nanotubes on the thermal properties of erythritol as phase change materials. Energ Convers Manage 2018;157:41-8. https://doi.org/10.1016/j.enconman.2017.11.072.

[43] Khosravi F, Montazer M. Facile preparation of fatty acids/nano [$Al(OH)_3$/Al_2O_3]/wool fabric introducing thermal energy management with multifunctional properties. J Energy Storage 2023;64:107170. https://doi.org/10.1016/j.est.2023.107170.

[44] Rezaie A B, Montazer M. One-step preparation of magnetically responsive nano $CuFe_2O_4$/fatty acids/polyester composite for dynamic thermal energy management applications. Renew Energ 2019;143:1839-51. https://doi.org/10.1016/j.renene.2019.05.132.

[45] Ma B J, Shin D, Banerjee D. One-step synthesis of molten salt nanofluid for thermal energy storage application - a comprehensive analysis on thermophysical property, corrosion behavior, and economic benefit. J Energy Storage 2021;35:102278. https://doi.org/10.1016/j.est.2021.102278.

[46] Liu Q Y, Xiao T, Zhao J T, Sun W J, Liu C H. Phase change thermal energy storage enabled by an In situ formed porous TiO_2. Small 2023;19:2204998. https://doi.org/10.1002/smll.202204998.

[47] Akhiani A R, Mehrali M, Latibari S T, Mehrali M, Mahlia T M I, Sadeghinezhad E, Metselaar H S C. One-step preparation of form-stable phase change material through self-assembly of fatty acid and graphene. J Phys Chem C 2015;119:22787-96. https://doi.org/10.1021/acs.jpcc.5b06089.

[48] Shang Y, Zhang D. Preparation and characterization of three-dimensional graphene network encapsulating 1-hexadecanol composite. Appl Therm Eng 2017;111:353-7. https://doi.org/10.1016/j.applthermaleng.2016.09.129.

[49] Yu W, Xie H Q. A Review on Nanofluids: preparation, stability mechanisms, and applications. J Nanomater 2012;2012:435873. https://doi.org/10.1155/2012/435873.

[50] Zeng J L, Zhu F R, Yu S B, Zhu L, Cao Z, Sun L X, Deng G R, Yan W P, Zhang L. Effects of copper nanowires on the properties of an organic phase change material. Sol Energ Mat Sol C 2012;105:174-8. https://doi.org/10.1016/j.solmat.2012.06.013.

[51] Wang N, Zhang X R, Zhu D S, Gao J W. The investigation of thermal conductivity and energy storage properties of graphite/paraffin composites. J Therm Anal Calorim 2012;107:949-54. https://doi.org/10.1007/s10973-011-1467-z.

[52] Fan L W, Zhu Z Q, Zeng Y, Xiao Y Q, Liu X L, Wu Y Y, Ding Q, Yu Z T, Cen K F. Transient performance of a PCM-based heat sink with high aspect-ratio carbon nanofillers. Appl Therm Eng 2015;75:532-40. https://doi.org/10.1016/j.applthermaleng.2014.10.050.

[53] Chinnasamy V, Cho H. Investigation on thermal properties enhancement of lauryl alcohol with multi-walled carbon nanotubes as phase change material for thermal energy storage. Case Stud Therm Eng 2022;31:101826. https://doi.org/10.1016/j.csite.2022.101826.

[54] Bharathiraja R, Ramkumar T, Selvakumar M. Studies on the thermal characteristics of nano-enhanced paraffin wax phase change material (PCM) for thermal storage applications. J Energy Storage 2023;73:109216. https://doi.org/10.1016/j.est.2023.109216.

[55] Tao Y B, Lin C H, He Y L. Preparation and thermal properties characterization of carbonate salt/carbon nanomaterial composite phase change material. Energ Convers Manage 2015;97:103-10. https://doi.org/10.1016/j.enconman.2015.03.051.

[56] Rufuss D D W, Suganthi L, Iniyan S, Davies P A. Effects of nanoparticle-enhanced phase change material (NPCM) on solar still productivity. J Clean Prod 2018;192:9-29. https://doi.org/10.1016/j.jclepro.2018.04.201.

[57] Praveen B, Suresh S. Experimental study on heat transfer performance of neopentyl glycol/CuO composite solid-solid PCM in TES based heat sink. Eng Sci Technol 2018;21:1086-94. https://doi.org/10.1016/j.jestch.2018.07.010.

[58] Tan Q L, Liu H F, Shi Y, Zhang M Y, Yu B D, Zhang Y. Lauric acid/stearic acid/nano-particles composite phase change materials for energy storage in buildings. J Energy Storage 2024;76:109664. https://doi.org/10.1016/j.est.2023.109664.

[59] Pandya M, Ansu A K, Sharma R K, Pandey A K, Tripathi D, Sari A, Tyagi V V. Development and laboratory scale characterization of a new hybrid nano-enhanced phase change material for solar thermal energy storage. Chemistryselect 2022;7:e202202709. https://doi.org/10.1002/slct.202202709.

[60] Sharma R K, Ganesan P, Tyagi V V, Metselaar H S C, Sandaran S C. Thermal properties and heat storage analysis of palmitic acid-TiO_2 composite as nano-enhanced organic phase change material (NEOPCM). Appl Therm Eng 2016;99:1254-62. https://doi.org/10.1016/j.applthermaleng.2016.01.130.

[61] Ho C J, Gao J Y. Preparation and thermophysical properties of nanoparticle-in-paraffin emulsion as phase change material. Int Commun Heat Mass 2009;36:467-70. https://doi.org/10.1016/j.icheatmasstransfer.2009.01.015.

[62] Lu B H, Zhang Y X, Zhang J Y, Zhu J J, Zhao H Y, Wang Z X. Preparation, optimization and thermal characterization of paraffin/nano-Fe_3O_4 composite phase change material for solar thermal energy storage. J Energy Storage 2022;46:103928. https://doi.org/10.1016/j.est.2021.103928.

[63] Saravanakumar P T, Arunkumar S P, Mansingh B B, Kumar P M, Subbiah R, Eswarlal V K. Investigating the effect of thermal cycling on thermal characteristics of the nano-silica based phase changing material (PCM). Mater Today-Proc 2022;50:1502-7. https://doi.org/10.1016/j.matpr.2021.09.095.

[64] Wu S Y, Zhu D S, Zhang X R, Huang J. Preparation and melting/freezing characteristics of Cu/Paraffin nanofluid as phase-change material (PCM). Energy & Fuels 2010;24:1894-8. https://doi.org/10.1021/ef9013967.

[65] Zabalegui A, Lokapur D, Lee H. Nanofluid PCMs for thermal energy storage: Latent heat reduction mechanisms and a numerical study of effective thermal storage performance. Int J Heat Mass Tran 2014;78:1145-54. https://doi.org/10.1016/j.ijheatmasstransfer.2014.07.051.

[66] Yu C J, Richter A G, Kmetko J, Dugan S W, Datta A, Dutta P. Structure of interfacial liquids: X-ray scattering studies. Phys Rev E 2001;63:021205. https://doi.org/10.1103/PhysRevE.63.021205.

[67] Xue L, Keblinski P, Phillpot S R, Choi S U S, Eastman J A. Effect of liquid layering at the liquid-solid interface on thermal transport. Int J Heat Mass Tran 2004;47:4277-84. https://doi.org/10.1016/j.ijheatmasstransfer.2004.05.016.

[68] Keblinski P, Phillpot S R, Choi S U S, Eastman J A. Mechanisms of heat flow in suspensions of nano-sized particles (nanofluids). Int J Heat Mass Tran 2002;45:855-63. https://doi.org/10.1016/S0017-9310(01)00175-2.

[69] Prasher R, Phelan P E, Bhattacharya P. Effect of aggregation kinetics on the thermal conductivity of nanoscale colloidal solutions (nanofluid). Nano Letters 2006;6:1529-34. https://doi.org/10.1021/nl060992s.

[70] Potanin A A, Russel W B. Fractal model of consolidation of weakly aggregated colloidal dispersions. Phys Rev E 1996;53:3702-9. https://doi.org/10.1103/PhysRevE.53.3702.

[71] Jiménez-Galea J J, Gómez-Merino A I. Fumed silica in coconut oil based nanofluids for cooling and lubrication in drilling applications. Lubricants 2024;12:436. https://doi.org/10.3390/lubricants12120436.

[72] Warzoha R J, Weigand R M, Fleischer A S. Temperature-dependent thermal properties of a paraffin phase change material embedded with herringbone style graphite nanofibers. Appl Energ 2015;137:716-25. https://doi.org/10.1016/j.apenergy.2014.03.091.

[73] Hayat M A, Yang Y Z, Li L, Bevilacqua M, Chen Y K. Preparation and thermophysical characterisation analysis of potential nano-phase transition materials for thermal energy storage applications. J Mol Liq 2023;376:121464. https://doi.org/10.1016/j.molliq.2023.121464.

[74] Karthikeyan K, Mariappan V, Kalidoss P, Ganesh J M J, Kishore P V R N, Prathiban S, Anish R. Characterization and thermal properties of lauryl alcohol-capric acid binary mixture with hybrid-nanoparticles as phase change material for vaccine storage applications. J Energy Storage 2023;74:109442. https://doi.org/10.1016/j.est.2023.109442.

[75] Avid A, Jafari S H, Khonakdar H A, Ghaffari M, Krause B, Pötschke P. Surface modification of MWCNT and its influence on properties of paraffin/MWCNT nanocomposites as phase change material. J Appl Polym Sci 2020;137:48428. https://doi.org/10.1002/app.48428.

[76] Sheikh Y, Orhan M F, Umair M, Mehaisi E, Azmeer A. Variation in cooling performance of a bio-based phase change material by adding graphene nanoplatelets with surfactants. International Journal of Thermofluids 2022;16:100201. https://doi.org/10.1016/j.ijft.2022.100201.

[77] Li J F, Lu W, Zeng Y B, Luo Z P. Simultaneous enhancement of latent heat and thermal conductivity of docosane-based phase change material in the presence of spongy graphene. Sol Energ Mat Sol C 2014;128:48-51. https://doi.org/10.1016/j.solmat.2014.05.018.

[78] Emeema J, Murali G, Reddi B V, Mangesh V L. Investigations on paraffin wax/CQD composite phase change material - Improved latent heat and thermal stability. J Energy Storage 2024;85:111056. https://doi.org/10.1016/j.est.2024.111056.

[79] Zaimi N H M, Nawabjan A, Rahman S F A, Hussin S M, Hamidon S N N A. Evaluating the role of sodium dodecylbenzene sulfonate as surfactant towards enhancing thermophysical properties of paraffin/graphene nanoplatelet phase change material: synthesis and characterization in PV cooling perspective. Int J Thermophys 2022;43:9. https://doi.org/10.1007/s10765-021-02931-9.

[80] Liu Y S, Yang Y Z. Investigation of specific heat and latent heat enhancement in hydrate salt based TiO_2 nanofluid phase change material. Appl Therm Eng 2017;124:533-8. https://doi.org/10.1016/j.applthermaleng.2017.05.150.

[81] Jacob J, Pandey A K, Abd Rahim N, Selvaraj J, Paul J, Samykano M, Saidur R. Quantifying thermophysical properties, characterization, and thermal cycle testing of nano-enhanced organic eutectic phase change materials for thermal energy storage applications. Sol Energ Mat Sol C 2022;248:112008. https://doi.org/10.1016/j.solmat.2022.112008.

[82] Aljaerani H A, Samykano M, Pandey A K, Said Z, Sudhakar K, Saidur R. Effect of TiO2 nanoparticles on the thermal energy storage of HITEC salt for concentrated solar power applications. J Energy Storage 2023;72:108449. https://doi.org/10.1016/j.est.2023.108449.

[83] Sahan N, Paksoy H O. Thermal enhancement of paraffin as a phase change material with nanomagnetite. Sol Energ Mat Sol C 2014;126:56-61. https://doi.org/10.1016/j.solmat.2014.03.018.

[84] Mohamed N H, Soliman F S, El Maghraby H, Moustfa Y M. Thermal conductivity enhancement of treated petroleum waxes, as phase change material, by a nano alumina: Energy storage. Renew Sust Energ Rev 2017;70:1052-8. https://doi.org/10.1016/j.rser.2016.12.009.

[85] Liu X, Rao Z H. Experimental study on the thermal performance of graphene and exfoliated graphite sheet for thermal energy storage phase change material. Thermochim Acta 2017;647:15-21. https://doi.org/10.1016/j.tca.2016.11.010.

[86] Sami S, Etesami N. Improving thermal characteristics and stability of phase change material containing TiO_2 nanoparticles after thermal cycles for energy storage. Appl Therm Eng 2017;124:346-52. https://doi.org/10.1016/j.applthermaleng.2017.06.023.

[87] Shaikh S, Lafdi K, Hallinan K. Carbon nanoadditives to enhance latent energy storage of phase change materials. J Appl Phys 2008;103:094302. https://doi.org/10.1063/1.2903538.

[88] Israelachvili J N. Intermolecular and surface forces, San Diego: Academic Press; 1994.

[89] Liu Y S, Yu K Y, Yang Y Z, Jia M J, Sun F Z. Size effects of nano-rutile TiO_2 on latent heat recovered of binary eutectic hydrate salt phase change material. Thermochim Acta 2020;684:178492. https://doi.org/10.1016/j.tca.2019.178492.

[90] Babaei H, Keblinski P, Khodadadi J M. Thermal conductivity enhancement of paraffins by increasing the alignment of molecules through adding CNT/graphene. Int J Heat Mass Tran 2013;58:209-16. https://doi.org/10.1016/j.ijheatmasstransfer.2012.11.013.

[91] Dsilva Winfred Rufuss D, Iniyan S, Suganthi L, Davies P A. Low mass fraction impregnation with graphene oxide (GO) enhances thermo-physical properties of paraffin for heat storage applications. Thermochim Acta 2017;655:226-33. https://doi.org/10.1016/j.tca.2017.07.005.

[92] Sutjahja I M, Anggraini Y, Yusuf A. Acceleration of heat discharge of composite lauric acid using magnetic dopant. J Energy Storage 2024;86:111219. https://doi.org/10.1016/j.est.2024.111219.

[93] Wang J F, Xie H Q, Guo Z X, Guan L H, Li Y. Improved thermal properties of paraffin wax by the addition of TiO_2 nanoparticles. Appl Therm Eng 2014;73:1541-7. https://doi.org/10.1016/j.applthermaleng.2014.05.078.

[94] Fang G, Zhao M, Sun P. Experimental study of the thermal properties of a fatty acid-modified graphite composite phase change material dispersion system. J Energy Storage 2022;53:105108. https://doi.org/10.1016/j.est.2022.105108.

[95] Yang Y Y, Luo J, Song G L, Liu Y, Tang G Y. The experimental exploration of nano-Si_3N_4/paraffin on thermal behavior of phase change materials. Thermochim Acta 2014;597:101-6. https://doi.org/10.1016/j.tca.2014.10.014.

[96] Wang B X, Zhou L P, Peng X F. Surface and size effects on the specific heat capacity of nanoparticles. Int J Thermophys 2006;27:139-51. https://doi.org/10.1007/s10765-006-0022-9.

[97] Faroughi S A, Huber C. Effective thermal conductivity of metal and non-metal particulate composites with interfacial thermal resistance at high volume fraction of nano to macro-sized spheres. J Appl Phys 2015;117:636-264. https://doi.org/10.1063/1.4907209.

[98] Li L, Zhang Y W, Ma H B, Yang M. Molecular dynamics simulation of effect of liquid layering around the nanoparticle on the enhanced thermal conductivity of nanofluids. J Nanopart Res 2010;12:811-21. https://doi.org/10.1007/s11051-009-9728-5.

[99] Oh S H, Kauffmann Y, Scheu C, Kaplan W D, Rühle M. Ordered liquid aluminum at the interface with sapphire. Science 2005;310:661-3. https://doi.org/10.1126/science.1118611.

[100] Yu Q, Zhang C C, Lu Y W, Kong Q L, Wei H J, Yang Y C, Gao Q, Wu Y T, Sciacovelli A. Comprehensive performance of composite phase change materials based on eutectic chloride with SiO_2 nanoparticles and expanded graphite for thermal energy storage system. Renew Energ 2021;172:1120-32. https://doi.org/10.1016/j.renene.2021.03.061.

[101] El Far B, Rizvi S M M, Nayfeh Y, Shin D. Investigation of heat capacity and viscosity enhancements of binary carbonate salt mixture with SiO_2 nanoparticles. Int J Heat Mass Tran 2020;156:119789. https://doi.org/10.1016/j.ijheatmasstransfer.2020.119789.

[102] Tiznobaik H, Shin D. Enhanced specific heat capacity of high-temperature molten salt-based nanofluids. Int J Heat Mass Tran 2013;57:542-8. https://doi.org/10.1016/j.ijheatmasstransfer.2012.10.062.

[103] Shin D, Banerjee D. Specific heat of nanofluids synthesized by dispersing alumina nanoparticles in alkali salt eutectic. Int J Heat Mass Tran 2014;74:210-4. https://doi.org/10.1016/j.ijheatmasstransfer.2014.02.066.

[104] Wu C L, Wang Q, Wang X M, Sun S P, Sun M Y, Zhang J H. Al_2O_3 nanoparticles for enhanced thermal performance in NaCl -KCl -Na_2CO_3 system: From thermodynamic prediction to system level assessment. Chem Eng J 2024;488 https://doi.org/10.1016/j.cej.2024.150789.

[105] Wu C L, Wang Q, Sun S P, Wang X M, Cui D, Pan S, Sheng H Y. Comprehensive thermal properties of ternary eutectic molten salt/nanoparticles composite phase change materials for high-temperature thermal energy storage. Sol Energ Mat Sol C 2023;261:112531. https://doi.org/10.1016/j.solmat.2023.112531.

[106] Xiao X, Jia H W, Wen D S, Zhao X D. Thermal performance analysis of a solar energy storage unit encapsulated with HITEC salt/copper foam/nanoparticles composite. Energy 2020;192:116593. https://doi.org/10.1016/j.energy.2019.116593.

[107] Aljaerani H A, Samykano M, Pandey A K, Kadirgama K, George M, Saidur R. Thermophysical properties enhancement and characterization of CuO nanoparticles enhanced HITEC molten salt for concentrated solar power applications. Int Commun Heat Mass 2022;132:105898. https://doi.org/10.1016/j.icheatmasstransfer.2022.105898.

[108] Chieruzzi M, Cerritelli G F, Miliozzi A, Kenny J M. Effect of nanoparticles on heat capacity of nanofluids based on molten salts as PCM for thermal energy storage. Nanoscale Res Lett 2013;8:448. https://doi.org/10.1186/1556-276x-8-448.

[109] He Q B, Wang S F, Tong M W, Liu Y D. Experimental study on thermophysical properties of nanofluids as phase-change material (PCM) in low temperature cool storage. Energ Convers Manage 2012;64:199-205. https://doi.org/10.1016/j.enconman.2012.04.010.

[110] Kumar A, Kothari R, Sahu S K, Kundalwal S I. Thermal performance of heat sink using nano-enhanced phase change material (NePCM) for cooling of electronic components. Microelectron Reliab 2021;121:114144. https://doi.org/10.1016/j.microrel.2021.114144.

[111] Liu X S, Marbut C, Huitink D, Feng G, Fleischer A S. Influence of crystalline polymorphism on the phase change properties of sorbitol-Au nanocomposites. Mater Today Energy 2019;12:379-88. https://doi.org/10.1016/j.mtener.2019.03.007.

[112] Luo Z C, Zhang Q, Wu G H. Preparation and enhanced heat capacity of nano-titania doped erythritol as phase change material. Int J Heat Mass Tran 2015;80:653-9. https://doi.org/10.1016/j.ijheatmasstransfer.2014.09.069.

[113] Aslfattahi N, Saidur R, Arifutzzaman A, Sadri R, Bimbo N, Sabri M F M, Maughan P A, Bouscarrat L, Dawson R J, Said S M, Goh B T, Sidik N A C. Experimental investigation of energy storage properties and thermal conductivity of a novel organic phase change material/MXene as A new class of nanocomposites. J Energy Storage 2020;27:101115. https://doi.org/10.1016/j.est.2019.101115.

[114] El-Sebaii A A, Aboul-Enein S, Ramadan M R I, Samy N, El-Sayed A R, Shalaby S M. Enhancing the thermal properties of paraffin wax as latent heat storage material using hybrid nanomaterials. Characterization and Application of Nanomaterials 2024;7:4912. https://doi.org/10.24294/can.v7i1.4912.

[115] Abdelrazik A S, Saidur R, Al-Sulaiman F A, Al-Ahmed A, Ben-Mansour R. Multiwalled CNT and graphene nanoplatelets based nano-enhanced PCMs: Evaluation for the thermal performance and its implications on the performance of hybrid PV/thermal systems. Mater Today Commun 2022;31:103618. https://doi.org/10.1016/j.mtcomm.2022.103618.

[116] Srinivasan S, Diallo M S, Saha S K, Abass O A, Sharma A, Balasubramanian G. Effect of temperature and graphite particle fillers on thermal conductivity and viscosity of phase change material -eicosane. Int J Heat Mass Tran 2017;114:318-23. https://doi.org/10.1016/j.ijheatmasstransfer.2017.06.081.

[117] Asadi A, Alarifi I M, Foong L K. An experimental study on characterization, stability and dynamic viscosity of CuO-TiO_2/water hybrid nanofluid. J Mol Liq 2020;307:112987. https://doi.org/10.1016/j.molliq.2020.112987.

[118] Brinkman H C. The viscosity of concentrated suspensions and solutions. The Journal of Chemical Physics 1952;20:571-. https://doi.org/10.1063/1.1700493.

[119] Motahar S, Nikkam N, Alemrajabi A A, Khodabandeh R, Toprak M S, Muhammed M. Experimental investigation on thermal and rheological properties of n-octadecane with dispersed TiO_2 nanoparticles. Int Commun Heat Mass 2014;59:68-74. https://doi.org/10.1016/j.icheatmasstransfer.2014.10.016.

[120] Motahar S, Nikkam N, Alemrajabi A A, Khodabandeh R, Toprak M S, Muhammed M. A novel phase change material containing mesoporous silica nanoparticles for thermal storage: A study on thermal conductivity and viscosity. Int Commun Heat Mass 2014;56:114-20. https://doi.org/10.1016/j.icheatmasstransfer.2014.06.005.

[121] Zhuang Y J, Liu Z B, Xu W B. Experimental investigation on the non-Newtonian to Newtonian rheology transition of nanoparticles enhanced phase change material during melting. Colloid Surface A 2021;629:127432. https://doi.org/10.1016/j.colsurfa.2021.127432.

[122] Delgado M, Lázar A, Peñalosa C, Zalba B. Experimental analysis of the influence of microcapsule mass fraction on the thermal and rheological behavior of a PCM slurry. Appl Therm Eng 2014;63:11-22. https://doi.org/10.1016/j.applthermaleng.2013.10.011.

[123] Yu Z T, Fang X, Fan L W, Wang X, Xiao Y Q, Zeng Y, Xu X, Hu Y C, Cen K F. Increased thermal conductivity of liquid paraffin-based suspensions in the presence of carbon nano-additives of various sizes and shapes. Carbon 2013;53:277-85. https://doi.org/10.1016/j.carbon.2012.10.059.

[124] Singh S K, Verma S K, Kumar R. Thermal performance and behavior analysis of SiO_2, Al_3O_4 and MgO based nano-enhanced phase-changing materials, latent heat thermal energy storage system. J Energy Storage 2022;48:103977. https://doi.org/10.1016/j.est.2022.103977.

[125] Harikrishnan S, Deenadhayalan M, Kalaiselvam S. Experimental investigation of solidification and melting characteristics of composite PCMs for building heating application. Energ Convers Manage 2014;86:864-72. https://doi.org/10.1016/j.enconman.2014.06.042.

[126] Nithiyanantham U, González-Fernández L, Grosu Y, Zaki A, Igartua J M, Faik A. Shape effect of Al_3O_4 nanoparticles on the thermophysical properties and viscosity of molten salt nanofluids for TES application at CSP plants. Appl Therm Eng 2020;169:114942. https://doi.org/10.1016/j.applthermaleng.2020.114942.

[127] Fang X, Ding Q, Li L Y, Moon K S, Wong C P, Yu Z T. Tunable thermal conduction character of graphite-nanosheets-enhanced composite phase change materials via cooling rate control. Energ Convers Manage 2015;103:251-8. https://doi.org/10.1016/j.enconman.2015.06.062.

[128] Zhu J, Wei S, Yadav A, Guo Z. Rheological behaviors and electrical conductivity of epoxy resin nanocomposites suspended with in-situ stabilized carbon nanofibers. Polymer 2010;51:2643-51. https://doi.org/10.1016/j.polymer.2010.04.019.

[129] Tuteja A, Duxbury P M, Mackay M E. Multifunctional nanocomposites with reduced viscosity. Macromolecules 2007;40:9427-34. https://doi.org/10.1021/ma071313i.

[130] Noori M M, Khonakdar H A, Azizi H, Ghaffari M, Arjmand M, Jafari S H. Paraffin/CuO nanocomposites as phase change materials: Effect of surface modification of CuO. Polym Composite 2019;40:4362-70. https://doi.org/10.1002/pc.25298.

[131] Lu W, Tassou S A. Experimental study of the thermal characteristics of phase change slurries for active cooling. Appl Energ 2012;91:366-74. https://doi.org/10.1016/j.apenergy.2011.10.004.

[132] Das N, Takata Y, Kohno M, Harish S. Effect of carbon nano inclusion dimensionality on the melting of phase change nanocomposites in vertical shell-tube thermal energy storage unit. Int J Heat Mass Tran 2017;113:423-31. https://doi.org/10.1016/j.ijheatmasstransfer.2017.05.101.

[133] Alazwari M A, Algarni M, Safaei M R. Effects of various types of nanomaterials on PCM melting process in a thermal energy storage system for solar cooling application using CFD and MCMC methods. Int J Heat Mass Tran 2022;195:123204. https://doi.org/10.1016/j.ijheatmasstransfer.2022.123204.

[134] Sun X Q, Liu L H, Mo Y J, Li J, Li C C. Enhanced thermal energy storage of a paraffin-based phase change material (PCM) using nano carbons. Appl Therm Eng 2020;181:115992. https://doi.org/10.1016/j.applthermaleng.2020.115992.

[135] Fan L W, Zhu Z Q, Zeng Y, Ding Q, Liu M J. Unconstrained melting heat transfer in a spherical container revisited in the presence of nano-enhanced phase change materials (NePCM). Int J Heat Mass Tran 2016;95:1057-69. https://doi.org/10.1016/j.ijheatmasstransfer.2016.01.013.

[136] Bahiraei F, Fartaj A, Nazri G A. Experimental and numerical investigation on the performance of carbon-based nanoenhanced phase change materials for thermal management applications. Energ Convers Manage 2017;153:115-28. https://doi.org/10.1016/j.enconman.2017.09.065.

[137] Lachachene F, Haddad Z, Oztop H F, Abu-Nada E. Melting of phase change materials in a trapezoidal cavity: Orientation and nanoparticles effects. J Mol Liq 2019;292:110592. https://doi.org/10.1016/j.molliq.2019.03.051.

[138] Zeng Y, Fan L W, Xiao Y Q, Yu Z T, Cen K F. An experimental investigation of melting of nanoparticle-enhanced phase change materials (NePCMs) in a bottom-heated vertical cylindrical cavity. Int J Heat Mass Tran 2013;66:111-7. https://doi.org/10.1016/j.ijheatmasstransfer.2013.07.022.

[139] Dhaidan N S, Khodadadi J M, Al-Hattab T A, Al-Mashat S M. Experimental and numerical investigation of melting of NePCM inside an annular container under a constant heat flux including the effect of eccentricity. Int J Heat Mass Tran 2013;67:455-68. https://doi.org/10.1016/j.ijheatmasstransfer.2013.08.002.

[140] Morimoto T, Togashi K, Kumano H, Hong H. Thermophysical properties of phase change emulsions prepared by D-phase emulsification. Energ Convers Manage 2016;122:215-22. https://doi.org/10.1016/j.enconman.2016.05.065.

[141] Chen J, Zhang P. Preparation and characterization of nano-sized phase change emulsions as thermal energy storage and transport media. Appl Energ 2017;190:868-79. https://doi.org/10.1016/j.apenergy.2017.01.012.

[142] Burger N, Laachachi A, Ferriol M, Lutz M, Toniazzo V, Ruch D. Review of thermal conductivity in composites: Mechanisms, parameters and theory. Prog Polym Sci 2016;61:1-28. https://doi.org/10.1016/j.progpolymsci.2016.05.001.

[143] Wu S F, Yan T, Kuai Z H, Pan W G. Thermal conductivity enhancement on phase change materials for thermal energy storage: A review. Energy Storage Mater 2020;25:251-95. https://doi.org/10.1016/j.ensm.2019.10.010.

[144] Kim W. Strategies for engineering phonon transport in thermoelectrics. J Mater Chem C 2015;3:10336-48. https://doi.org/10.1039/c5tc01670c.

[145] Mehra N, Mu L W, Ji T, Yang X T, Kong J, Gu J W, Zhu J H. Thermal transport in polymeric materials and across composite interfaces. Appl Mater Today 2018;12:92-130. https://doi.org/10.1016/j.apmt.2018.04.004.

[146] Kim Y A, Kamio S, Tajiri T, Hayashi T, Song S M, Endo M, Terrones M, Dresselhaus M S. Enhanced thermal conductivity of carbon fiber/phenolic resin composites by the introduction of carbon nanotubes. Appl Phys Lett 2007;90:093125. https://doi.org/10.1063/1.2710778.

[147] Song Z Y, Hou X X, Zhang L Q, Wu S Z. Enhancing crystallinity and orientation by hot-stretching to improve the mechanical properties of electrospun partially aligned polyacrylonitrile (PAN) nanocomposites. Materials 2011;4:621-32. https://doi.org/10.3390/ma4040621.

[148] Weisenberger M, Martin-Gullon I, Vera-Agullo J, Varela-Rizo H, Merino C, Andrews R, Qian D L, Rantell T. The effect of graphitization temperature on the structure of helical-ribbon carbon nanofibers. Carbon 2009;47:2211-8. https://doi.org/10.1016/j.carbon.2009.03.070.

[149] Lim S, Yoon S H, Mochida I, Chi J H. Surface modification of carbon nanofiber with high degree of graphitization. J Phys Chem B 2004;108:1533-6. https://doi.org/10.1021/jp036819r.

[150] Zeng J L, Cao Z, Yang D W, Sun L X, Zhang L. Thermal conductivity enhancement of Ag nanowires on an organic phase change material. J Therm Anal Calorim 2010;101:385-9. https://doi.org/10.1007/s10973-009-0472-y.

[151] Ganguli S, Roy A K, Anderson D P. Improved thermal conductivity for chemically functionalized exfoliated graphite/epoxy composites. Carbon 2008;46:806-17. https://doi.org/10.1016/j.carbon.2008.02.008.

[152] Yuan P, Zhang P, Liang T, Zhai S P, Yang D G. Effects of functionalization on energy storage properties and thermal conductivity of graphene/n-octadecane composite phase change materials. J Mater Sci 2019;54:1488-501. https://doi.org/10.1007/s10853-018-2883-2.

[153] Lv C, Xue Q Z, Xia D, Ma M, Xie J, Chen H J. Effect of chemisorption on the interfacial bonding characteristics of graphene-polymer composites. J Phys Chem C 2010;114:6588-94. https://doi.org/10.1021/jp100110n.

[154] Huang Y R, Chuang P H, Chen C L. Molecular-dynamics calculation of the thermal conduction in phase change materials of graphene paraffin nanocomposites. Int J Heat Mass Tran 2015;91:45-51. https://doi.org/10.1016/j.ijheatmasstransfer.2015.07.110.

[155] Kim J Y, Lee J H, Grossman J C. Thermal transport in functionalized graphene. Acs Nano 2012;6:9050-7. https://doi.org/10.1021/nn3031595.

[156] Mortazavi B, Ahzi S. Thermal conductivity and tensile response of defective graphene: A molecular dynamics study. Carbon 2013;63:460-70. https://doi.org/10.1016/j.carbon.2013.07.017.

[157] Gulotty R, Castellino M, Jagdale P, Tagliaferro A, Balandin A A. Effects of Functionalization on Thermal Properties of Single-Wall and Multi-Wall Carbon Nanotube-Polymer Nanocomposites. Acs Nano 2013;7:5114-21. https://doi.org/10.1021/nn400726g.

[158] Liu C H, Fan S S. Effects of chemical modifications on the thermal conductivity of carbon nanotube composites. Appl Phys Lett 2005;86:123106. https://doi.org/10.1063/1.1887839.

[159] Park J G, Cheng Q F, Lu J, Bao J W, Li S, Tian Y, Liang Z Y, Zhang C, Wang B. Thermal conductivity of MWCNT/epoxy composites: The effects of length, alignment and functionalization. Carbon 2012;50:2083-90. https://doi.org/10.1016/j.carbon.2011.12.046.

[160] Xiang J L, Drzal L T. Investigation of exfoliated graphite nanoplatelets (GnP) in improving thermal conductivity of paraffin wax-based phase change material. Sol Energ Mat Sol C 2011;95:1811-8. https://doi.org/10.1016/j.solmat.2011.01.048.

[161] Luo T F, Lloyd J R. Enhancement of thermal energy transport across graphene/graphite and polymer interfaces: A molecular dynamics study. Adv Funct Mater 2012;22:2495-502. https://doi.org/10.1002/adfm.201103048.

[162] Debelak B, Lafdi K. Use of exfoliated graphite filler to enhance polymer physical properties. Carbon 2007;45:1727-34. https://doi.org/10.1016/j.carbon.2007.05.010.

[163] Su J F, Zhao Y H, Wang X Y, Dong H, Wang S B. Effect of interface debonding on the thermal conductivity of microencapsulated-paraffin filled epoxy matrix composites. Compos Part a-Appl S 2012;43:325-32. https://doi.org/10.1016/j.compositesa.2011.12.003.

[164] Zhu B L, Wang J, Zheng H, Ma J, Wu J, Wu R. Investigation of thermal conductivity and dielectric properties of LDPE-matrix composites filled with hybrid filler of hollow glass microspheres and nitride particles. Compos Part B-Eng 2015;69:496-506. https://doi.org/10.1016/j.compositesb.2014.10.035.

[165] Goli P, Legedza S, Dhar A, Salgado R, Renteria J, Balandin A A. Graphene-enhanced hybrid phase change materials for thermal management of Li-ion batteries. J Power Sources 2014;248:37-43. https://doi.org/10.1016/j.jpowsour.2013.08.135.

[166] Yu A P, Ramesh P, Itkis M E, Bekyarova E, Haddon R C. Graphite nanoplatelet-epoxy composite thermal interface materials. J Phys Chem C 2007;111:7565-9. https://doi.org/10.1021/jp071761s.

[167] Fan L W, Fang X, Wang X, Zeng Y, Xiao Y Q, Yu Z T, Xu X, Hu Y C, Cen K F. Effects of various carbon nanofillers on the thermal conductivity and energy storage properties of paraffin-based nanocomposite phase change materials. Appl Energ 2013;110:163-72. https://doi.org/10.1016/j.apenergy.2013.04.043.

[168] Prado J I, Lugo L. Enhancing the thermal performance of a stearate phase change material with graphene nanoplatelets and MgO nanoparticles. Acs Appl Mater Inter 2020;12:39108-17. https://doi.org/10.1021/acsami.0c09643.

[169] He M Z, Yang L W, Lin W Y, Chen J X, Mao X, Ma Z J. Preparation, thermal characterization and examination of phase change materials (PCMs) enhanced by carbon-based nanoparticles for solar thermal energy storage. J Energy Storage 2019;25:100874. https://doi.org/10.1016/j.est.2019.100874.

[170] Bharathiraja R, Ramkumar T, Selvakumar M, Radhika N. Thermal characteristics enhancement of paraffin wax phase change material (PCM) for thermal storage applications. Renew Energ 2024;222:119986. https://doi.org/10.1016/j.renene.2024.119986.

[171] Sathishkumar A S, Balasubramanian K A, Ramkumar T. Investigations on thermal properties of MWCNT-NBN Paraffin Wax phase change material for thermal storage applications. J Therm Anal Calorim 2023;148:3263-71. https://doi.org/10.1007/s10973-022-11931-2.

[172] Arshad A, Jabbal M, Shi L, Yan Y Y. Thermophysical characteristics and enhancement analysis of carbon-additives phase change mono and hybrid materials for thermal management of electronic devices. J Energy Storage 2021;34:102232. https://doi.org/10.1016/j.est.2020.102231.

[173] Chen G J, Su Y P, Jiang D Y, Pan L J, Li S. An experimental and numerical investigation on a paraffin wax/graphene oxide/carbon nanotubes composite material for solar thermal storage applications. Appl Energ 2020;264:114786. https://doi.org/10.1016/j.apenergy.2020.114786.

[174] Tong X Y, Li D, Yang R T, Arici M, Wu Y Y, Liu C Y, Yildiz Ç. Experimental investigation on photothermal properties of Zn-ZnO/paraffin hybrid nanofluids. J Therm Anal Calorim 2023;148:11029-40. https://doi.org/10.1007/s10973-023-12310-1.

[175] Evans W, Fish J, Keblinski P. Role of Brownian motion hydrodynamics on nanofluid thermal conductivity. Appl Phys Lett 2006;88:093116. https://doi.org/10.1063/1.2179118.

[176] Xie H Q, Fujii M, Zhang X. Effect of interfacial nanolayer on the effective thermal conductivity of nanoparticle-fluid mixture. Int J Heat Mass Tran 2005;48:2926-32. https://doi.org/10.1016/j.ijheatmasstransfer.2004.10.040.

[177] Leong K C, Yang C, Murshed S M S. A model for the thermal conductivity of nanofluids - the effect of interfacial layer. J Nanopart Res 2006;8:245-54. https://doi.org/10.1007/s11051-005-9018-9.

[178] Zhao C Y, Yang C, Tao Y B, He Y L. Interfacial nanolayer effect on thermophysical properties of silica-paraffin phase change material - A molecular dynamics simulation. Int J Heat Mass Tran 2024;220:125007. https://doi.org/10.1016/j.ijheatmasstransfer.2023.125007.

[179] Arshad A, Jabbal M, Shi L, Darkwa J, Weston N J, Yan Y Y. Development of TiO_2/RT-35HC based nanocomposite phase change materials (NCPCMs) for thermal management applications. Sustainable Energy Technologies and Assessments 2021;43:100865. https://doi.org/10.1016/j.seta.2020.100865.

[180] Gao J W, Zheng R T, Ohtani H, Zhu D S, Chen G. Experimental investigation of heat conduction mechanisms in nanofluids clue on clustering. Nano Letters 2009;9:4128-32. https://doi.org/10.1021/nl902358m.

[181] Singh R P, Sze J Y, Kaushik S C, Rakshit D, Romagnoli A. Thermal performance enhancement of eutectic PCM laden with functionalised graphene nanoplatelets for an efficient solar absorption cooling storage system. J Energy Storage 2021;33:102092. https://doi.org/10.1016/j.est.2020.102092.

[182] Dhaidan N S, Khodadadi J M, Al-Hattab T A, Al-Mashat S M. Experimental and numerical investigation of melting of phase change material/nanoparticle suspensions in a square container subjected to a constant heat flux. Int J Heat Mass Tran 2013;66:672-83. https://doi.org/10.1016/j.ijheatmasstransfer.2013.06.057.

[183] Jesumathy S, Udayakumar M, Suresh S. Experimental study of enhanced heat transfer by addition of CuO nanoparticle. Heat Mass Transfer 2012;48:965-78. https://doi.org/10.1007/s00231-011-0945-y.

[184] Wang J F, Xie H Q, Xin Z, Li Y, Yin C. Investigation on thermal properties of heat storage composites containing carbon fibers. J Appl Phys 2011;110:094302. https://doi.org/10.1063/1.3656991.

[185] Li M, Chen M R, Wu Z S, Liu J X. Carbon nanotube grafted with polyalcohol and its influence on the thermal conductivity of phase change material. Energ Convers Manage 2014;83:325-9. https://doi.org/10.1016/j.enconman.2014.04.002.

[186] Rebrovic L, Jukic A, Faraguna F. Influence of MWCNTs geometry and surface oxidation on rheological and thermal properties of PEG nanofluids. J Therm Anal Calorim 2023;148:1351-64. https://doi.org/10.1007/s10973-022-11558-3.

[187] Kumar P M, Anandkumar R, Sudarvizhi D, Mylsamy K, Nithish M. Experimental and theoretical Investigations on thermal conductivity of the paraffin wax using CuO nanoparticles. Mater Today-Proc 2020;22:1987-93. https://doi.org/10.1016/j.matpr.2020.03.164.

[188] Masoumi H, Khoshkhoo R H. Investigation of melting of nanoparticle-enhanced phase change materials (NePCMs) in a shell-and-tube heat exchanger with longitudinal fins. Heat Mass Transfer 2021;57:681-701. https://doi.org/10.1007/s00231-020-02983-x.

[189] Harish S, Orejon D, Takata Y, Kohno M. Thermal conductivity enhancement of lauric acid phase change nanocomposite in solid and liquid state with single-walled carbon nanohorn inclusions. Thermochim Acta 2015;600:1-6. https://doi.org/10.1016/j.tca.2014.12.004.

[190] Al Ghossein R M, Hossain M S, Khodadadi J M. Experimental determination of temperature-dependent thermal conductivity of solid eicosane-based silver nanostructure-enhanced phase change materials for thermal energy storage. Int J Heat Mass Tran 2017;107:697-711. https://doi.org/10.1016/j.ijheatmasstransfer.2016.11.059.

[191] Wang J F, Xie H Q, Xin Z, Li Y, Chen L F. Enhancing thermal conductivity of palmitic acid based phase change materials with carbon nanotubes as fillers. Sol Energy 2010;84:339-44. https://doi.org/10.1016/j.solener.2009.12.004.

[192] Nourani M, Hamdami N, Keramat J, Moheb A, Shahedi M. Thermal behavior of paraffin-nano-Al_2O_3 stabilized by sodium stearoyl lactylate as a stable phase change material with high thermal conductivity. Renew Energ 2016;88:474-82. https://doi.org/10.1016/j.renene.2015.11.043.

[193] Wang J F, Xie H Q, Xin Z, Li Y. Increasing the thermal conductivity of palmitic acid by the addition of carbon nanotubes. Carbon 2010;48:3979-86. https://doi.org/10.1016/j.carbon.2010.06.044.

[194] Wang J F, Xie H Q, Xin Z. Thermal properties of paraffin based composites containing multi-walled carbon nanotubes. Thermochim Acta 2009;488:39-42. https://doi.org/10.1016/j.tca.2009.01.022.

[195] Qian T T, Li J H, Feng W W, Nian H E. Single-walled carbon nanotube for shape stabilization and enhanced phase change heat transfer of polyethylene glycol phase change material. Energ Convers Manage 2017;143:96-108. https://doi.org/10.1016/j.enconman.2017.03.065.

[196] Krishna J, Kishore P S, Solomon A B. Heat pipe with nano enhanced-PCM for electronic cooling application. Exp Therm Fluid Sci 2017;81:84-92. https://doi.org/10.1016/j.expthermflusci.2016.10.014.

[197] Wu S Y, Wang H, Xiao S, Zhu D S. An investigation of melting/freezing characteristics of nanoparticle-enhanced phase change materials. J Therm Anal Calorim 2012;110:1127-31. https://doi.org/10.1007/s10973-011-2080-x.

[198] Gao L, Fan X H, Zhang S X, Che D Y, Sun B Z. Palmitic acid graphene composite phase change materials: A molecular dynamics simulation. Thermochim Acta 2022;707:179095. https://doi.org/10.1016/j.tca.2021.179095.

[199] Samykano M. Advancing battery thermal management: Future directions and challenges in nano-enhanced phase change materials-Based systems. Prog Mater Sci 2025;148:101388. https://doi.org/10.1016/j.pmatsci.2024.101388.

[200] Kumar R, Mitra A, Srinivas T. Role of nano-additives in the thermal management of lithium-ion batteries: A review. J Energy Storage 2022;48:104059. https://doi.org/10.1016/j.est.2022.104059.

[201] Yang L, Zhou F J, Sun L, Wang S Y. Thermal management of lithium-ion batteries with nanofluids and nano-phase change materials: a review. J Power Sources 2022;539:231605. https://doi.org/10.1016/j.jpowsour.2022.231605.

[202] Keshteli A N, Sheikholeslami M. Nanoparticle enhanced PCM applications for intensification of thermal performance in building: A review. J Mol Liq 2019;274:516-33. https://doi.org/10.1016/j.molliq.2018.10.151.

[203] Ma Z J, Lin W Y, Sohel M I. Nano-enhanced phase change materials for improved building performance. Renew Sust Energ Rev 2016;58:1256-68. https://doi.org/10.1016/j.rser.2015.12.234.

[204] Mourad A, Aissa A, Said Z, Younis O, Iqbal M, Alazzam A. Recent advances on the applications of phase change materials for solar collectors, practical limitations, and challenges: A critical review. J Energy Storage 2022;49:104186. https://doi.org/10.1016/j.est.2022.104186.

[205] Wang Q R, Yang L, Song J Z. Preparation, thermal conductivity, and applications of nano-enhanced phase change materials (NEPCMs) in solar heat collection: A review. J Energy Storage 2023;63:107047. https://doi.org/10.1016/j.est.2023.107047.

[206] Ali F H, Al-amir Q R, Hamzah H K, Alahmer A. Integrating thermal phase-change material energy storage with solar collectors: A comprehensive review of techniques and applications. Int Commun Heat Mass 2025;162:108606. https://doi.org/10.1016/j.icheatmasstransfer.2025.108606.

[207] Zarei M, Vahidhosseini S M, Rashidi S, Rafee R, Yan W M. Review on the efficiency enhancement of solar-assisted heat pumps using nano-enhanced phase change materials (NEPCM). J Energy Storage 2025;114:115804. https://doi.org/10.1016/j.est.2025.115804.

[208] Hinojosa J F, Moreno S F, Maytorena V M. Low-temperature applications of phase change materials for energy storage: A descriptive review. Energies 2023;16:3078. https://doi.org/10.3390/en16073078.

[209] Kumar R R, Samykano M, Pandey A K, Kadirgama K, Tyagi V V. Phase change materials and nano-enhanced phase change materials for thermal energy storage in photovoltaic thermal systems: A futuristic approach and its technical challenges. Renew Sust Energ Rev 2020;133:110341. https://doi.org/10.1016/j.rser.2020.110341.

[210] Tyagi P K, Kumar R, Said Z. Recent advances on the role of nanomaterials for improving the performance of photovoltaic thermal systems: Trends, challenges and prospective. Nano Energy 2022;93:106834. https://doi.org/10.1016/j.nanoen.2021.106834.

[211] Yuan Y P, Zhang N, Tao W Q, Cao X L, He Y L. Fatty acids as phase change materials: A review. Renew Sust Energ Rev 2014;29:482-98. https://doi.org/10.1016/j.rser.2013.08.107.

[212] Hu Y P, Yang J, Tian J W, Jia L, Yu J S. Green and size-controllable synthesis of photoluminescent carbon nanoparticles from waste plastic bags. Rsc Adv 2014;4:47169-76. https://doi.org/10.1039/c4ra08306g.

[213] Rajarao R, Ferreira R, Sadi S H F, Khanna R, Sahajwalla V. Synthesis of silicon carbide nanoparticles by using electronic waste as a carbon source. Mater Lett 2014;120:65-8. https://doi.org/10.1016/j.matlet.2014.01.018.

[214] Khalil N M. Exploitation of the ceramic wastes for the extraction of nano aluminum oxide powder. J Ind Eng Chem 2014;20:3663-6. https://doi.org/10.1016/j.jiec.2013.12.063.

[215] Ding H, Li J Q, Gao Y J, Zhao D, Shi D J, Mao G Z, Liu S J, Tan X. Preparation of silica nanoparticles from waste silicon sludge. Powder Technology 2015;284:231-6. https://doi.org/10.1016/j.powtec.2015.06.063.

[216] Na S H, Shon H K, Kim J B, Park H J, Kim J H. Preparation and characterization of titania nanoparticle produced from Ti-flocculated sludge with paper mill wastewater. J Ind Eng Chem 2011;17:277-81. https://doi.org/10.1016/j.jiec.2011.02.022.

[217] Huang R X, Fang Z Q, Fang X B, Tsang E P. Ultrasonic Fenton-like catalytic degradation of bisphenol A by ferroferric oxide (Fe_3O_4) nanoparticles prepared from steel pickling waste liquor. J Colloid Interf Sci 2014;436:258-66. https://doi.org/10.1016/j.jcis.2014.08.035.

[218] Hassan T A, Rangari V K, Jeelani S. Mechanical and thermal properties of bio-based $CaCO_3$/soybean-based hybrid unsaturated polyester nanocomposites. J Appl Polym Sci 2013;130:1442-52. https://doi.org/10.1002/app.39227.

[219] Rangari V K, Apalangya V, Biswas M, Jeelani S. Preparation and microscopic characterization of biobased nanoparticles from natural waste materials. Microsc and Microanal 2017;23:1938-9. https://doi.org/10.1017/s1431927617010352.

[220] Heuss-Aßbichler S, John M, Klapper D, Bläß U W, Kochetov G. Recovery of copper as zero-valent phase and/or copper oxide nanoparticles from wastewater by ferritization. J Environ Manage 2016;181:1-7. https://doi.org/10.1016/j.jenvman.2016.05.053.

[221] Swain B, Shin D, Joo S Y, Ahn N K, Lee C G, Yoon J H. Selective recovery of silver from waste low-temperature co-fired ceramic and valorization through silver nanoparticle synthesis. Waste Manage 2017;69:79-87. https://doi.org/10.1016/j.wasman.2017.08.024.

[222] Yousef S, Hamdy M, Tatariants M, Tuckute S, El-Abden S Z, Kliucininkas L, Baltusnikas A. Sustainable industrial technology for recovery of cellulose from banknote production waste and reprocessing into cellulose nanocrystals. Resour Conserv Recy 2019;149:510-20. https://doi.org/10.1016/j.resconrec.2019.06.026.

[223] Yousefi A, Tang W C, Khavarian M, Fang C, Wang S Y. Thermal and mechanical properties of cement mortar composite containing recycled expanded glass aggregate and nano titanium dioxide. Appl Sci-Basel 2020;10:2246. https://doi.org/10.3390/app10072246.

[224] Islam M M, Hasanuzzaman M, Rahim N A, Pandey A K, Rawa M, Kumar L. Real time experimental performance investigation of a NePCM based photovoltaic thermal system: An energetic and exergetic approach. Renew Energ 2021;172:71-87. https://doi.org/10.1016/j.renene.2021.02.169.

[225] Al-Kayiem H H, Lin S C. Performance evaluation of a solar water heater integrated with a PCM nanocomposite TES at various inclinations. Sol Energy 2014;109:82-92. https://doi.org/10.1016/j.solener.2014.08.021.

[226] Said Z, Sohail M A, Pandey A K, Sharma P, Waqas A, Chen W H, Nguyen P Q P, Nguyen V N, Pham N D K, Nguyen X P. Nanotechnology-integrated phase change material and nanofluids for solar applications as a potential approach for clean energy strategies: Progress, challenges, and opportunities. J Clean Prod 2023;416:137736. https://doi.org/10.1016/j.jclepro.2023.137736.

[227] Al-Waeli A H A, Kazem H A, Chaichan M T, Sopian K. Experimental investigation of using nano-PCM/nanofluid on a photovoltaic thermal system (PVT): Technical and economic study. Therm Sci Eng Prog 2019;11:213-30. https://doi.org/10.1016/j.tsep.2019.04.002.

[228] Yousefi A, Tang W C, Khavarian M, Fang C. Development of novel form-stable phase change material (PCM) composite using recycled expanded glass for thermal energy storage in cementitious composite. Renew Energ 2021;175:14-28. https://doi.org/10.1016/j.renene.2021.04.123.

[229] Rajamony R K, Pandey A K, Sofiah A G N, Wadaan M A, Paw J K S, Suraparaju S K, Baabbad A, Samykano M, Paranthaman V. Energy, exergy, economic and environmental (4E) analysis of serpentine tube absorber photovoltaic thermal system using nano enhanced phase change material. Energy 2025;319:135032. https://doi.org/10.1016/j.energy.2025.135032.

[230] El Qattan A. Enhancing an urban energy efficiency by application of PCM and nano- PCM materials in residential building, In Proceedings of the 12th International Conference on Nano-Technology for Green and Sustainable Construction. Sharm El-Sheikh; 2020.